Flexoelectric Effect in Solids

Pavlo Zubko

Department of Condensed Matter Physics, University of Geneva, Geneva 1211, Switzerland

email: pavlo.zubko@unige.ch

Gustau Catalan

Institut Català de Recerca I Estudis Avanats (ICREA), Catalunya, Spain

Institut Català de Nanocincia i Nanotecnologia (ICN2), CSIC-ICN, Campus Universitat Autonoma de Barcelona, Spain

email: gustau.catalan@cin2.es

Alexander K. Tagantsev

Ceramics Laboratory, Swiss Federal Institute of Technology (EPFL), Lausanne 1015, Switzerland

email: alexander.tagantsev@epfl.ch

Key Words strain gradients, electromechanical coupling, piezoelectricity, ferroelectricity, domain walls

Abstract Piezoelectricity—the coupling between strain and electrical polarization, allowed

by symmetry in a restricted class of materials—is at the heart of many devices that permeate our daily life. Since its discovery in the 1880's by Pierre and Jacques Curie, the piezoelectric effect has found use in everything from submarine sonars to cigarette lighters. By contrast, flexoelectricity—the coupling between polarization and strain gradients, allowed by symmetry in all materials—was largely overlooked for decades since its first proposal in the late 1950's, due to the seemingly small magnitude of the effect in bulk. The development of nanoscale technologies, however, has renewed the interest in flexoelectricity, as the large strain gradients often present at the nanoscale can lead to dramatic flexoelectric phenomena. Here we review the fundamentals of the flexoelectric effect, discuss its presence in many nanoscale systems, and look at potential applications of this fascinating phenomenon. The review will also emphasize the many open questions and unresolved issues in this developing field.

Contents

1 Introduction

Flexoelectricity is a property of all insulators whereby they polarize when subject to an inhomogeneous deformation. The flexoelectric coupling is between polarization and strain *gradient*, rather than homogeneous strain, and this difference is crucial to understand both the advantages and the limitations of flexoelectricity as compared to its close relative, piezoelectricity.

Strain, like stress, does not by itself break centrosymmetry: if a material is centrosymmetric to start with, it will continue to be centrosymmetric under a homogeneous deformation. This is intuitively clear: when a plate of a centrosymmetric material is subjected to a homogenous deformation (**Figure 1a**) we cannot rationalize the appearance of polarization since there is no preferred sense of direction for the polarization vector. By contrast, a strain gradient does break centrosymmetry. Under a strain gradient (e.g., resulting from bending, as in **Figure 1b**), the top and bottom surfaces of the plate are no longer equivalent and therefore define a sense of direction for the induced polarization vector. Mathematically, the flexoelectric effect is controlled by a fourth rank tensor and is therefore allowed in materials of any symmetry, whereas piezoelectricity is controlled by a third rank tensor, which is allowed only in materials that are non-centrosymmetric; their polarization occurs due to the low symmetry of the material rather than the symmetry-breaking effect of the perturbation.

Flexoelectricity as a strain-gradient-driven breaking of the local centrosymmetry can also be visualized at the microscopic level. For a simple ionic lattice, such as that sketched in **Figure 1b**, a vertical gradient of in-plane strain (induced, for instance, by bending) may cause the central cation to shift up like a pea inside a pea-pod, breaking the local centrosymmetry and inducing polarity.

Though this analogy, based purely on steric considerations, is quite crude, it is actually close to the idea of Bursian and Zaikovskii [1] that the central Ti ion in the ferroelectric perovskite $BaTiO_3$ must shift up on bending, or, vice-versa, that bending must appear due to the presence of a Ti ion in the upper side of the unit cell, which causes it to expand while the "emptier" lower half contracts. An alternative picture is provided by Harris [2], who noticed that the strain gradient in a shock-wave makes unequal the distances between the atomic planes of a centrosymmetric material, resulting in a local breaking of centrosymmetry.

The above are all simple ionic pictures, with rigid ions shifting and causing polarization. The flexoelectric effect is nevertheless a subtle physical phenomenon and its intuitive vision is often deceptive. For example, the conclusion about the sign of the flexoelectric response that one might draw for the cartoon shown in **Figure 1b** may readily be wrong [3, 4].

Of course, strain gradients affect not only ionic positions — an asymmetric redistribution of electron density will take place as well, contributing to the total polarization. The flexoelectricity in graphene [5] is controlled by this mechanism. The ionic and electronic components of flexoelectricity are complementary, but in this article we will keep an ionic picture for simplicity. We also exclude from this article the flexoelectricity of liquid crystals [6] (which is actually the field where the term "flexoelectricity" was first coined) and biological materials [7–9], as they originate from different physics and have very different applications.

So why should we care about flexoelectricity? Electromechanical properties play an essential role in the physics of solids and their practical application. Until recently, when referring to electromechanical properties, one generally meant piezoelectricity and electrostricition, whereas flexoelectricity was hardly men-

tioned on account of its relative weakness. However, it is becoming clear that this neglect is not justified, for several reasons. First, flexoelectricity, in contrast to piezoelectricity, is a universal property allowed by symmetry in any structure, and this broadens the choice of materials that can be used for electromechanical sensors and actuators. Second, reduced dimensions imply larger gradients: a strain difference over a small distance gives a large strain gradient. The small length scales involved in nanotechnology thus lead to a growing impact of flexoelectricity, which at the nanoscale may even be competitive with piezoelectricity. In addition, a number of experiments have reported giant flexoelectric coupling constants, exceeding theoretical estimates by several orders of magnitude. Finally, the polar nature of the flexoelectric effect means that strain gradients can effectively play the role of an equivalent electric field and can be used, for example, to switch the spontaneous polarization of a ferroelectric material. By contrast, switching of polarization by homogeneous strain is generally forbidden by symmetry and is only possible in special cases, such as when the paraelectric phase is also piezoelectric. What this means is that flexoelectricity is not just a substitute of piezoelectricity at the nanoscale, but it enables additional electromechanical functionalities not available otherwise.

Several excellent reviews, focusing primarily on flexoelectricity in bulk materials, have alredy been published and the reader is referred to Refs. 3, 4, 10–12. The subject is, however, evolving very rapidly, with many new developments happening in the last few years, particularly in the area of nanoscale materials such as thin films. We will therefore focus more attention on recent developments, both in experiment and theory, as well as on controversial or unresolved issues. We will begin with a brief introduction to the phenomenological theory

of bulk flexoelectricity in section 2, where many of the characteristic features of flexoelectricity will be derived. The concepts discussed here will be referred to throughout the rest of the review. In section 4, we then turn our attention to the magnitude of the flexoelectric response and discuss the progress made and challenges faced in the development of a microscopic theory of flexoelectricity. Section 5 is devoted to experimental studies of flexoelectricity in both bulk and nanoscale materials, and section 6 addresses possible applications based on the flexoelectric effect. Finally, we conclude this review with a brief summary of open questions and proposed future research in section 7.

2 Basic phenomenological description of the bulk effect

Theoretical work on flexoelectricity dates back to the seminal papers by Mashkevich and Tolpygo, who first proposed the effect [13, 14], and Kogan, who formulated the first phenomenological theory [15]. For a historical overview of the early developments in the theory of flexoelectricity the reader is referred to the comprehensive review by Tagantsev [4] as well as the more recent, concise summary by Maranganti *et al.* [11]. Here we will briefly summarize the basic phenomenological description of the direct and converse flexoelectric effects, emphasizing the differences from piezoelectricity and the analogies between strain gradients and electric fields.

2.1 Static response

2.1.1 Constitutive Equations In contrast to the piezoelectric response, the treatment of the flexoelectric effect in the static (e.g. in a bent plate) and dynamic (in a sound wave) situations generally requires separate treatments [4,

16]. Let us start with the static case.

We introduce this effect as a linear response of polarization P_i to a strain gradient $\partial u_{kl}/\partial x_j$ in the absence of electric field. It is governed by a fourth rank *flexoelectric tensor*, μ_{ijkl}:

$$\mu_{klij} = \left(\frac{\partial P_i}{\partial \left(\partial u_{kl}/\partial x_j \right)} \right)_{E=0} \tag{1}$$

where E stands for the electric field. This effect can readily be incorporated into the Landau phenomenological framework. Despite the need for tensors for the description of the flexoelectricity, an insight into this phenomenon can be gained by considering a one-dimensional model involving one component of polarization and one of strain, where the tensor suffixes can be omitted.

In such a model, the macroscopic description of the static bulk flexoelectric response can be obtained by generalizing the thermodynamic potential, used for the description of the piezoelectric response, by introducing a linear coupling between the polarization and strain gradient and visa versa into the system. In the most general form, a thermodynamic potential density suitable for such a description reads

$$\Phi_G = \frac{1}{2\chi} P^2 + \frac{c}{2} u^2 - \vartheta P u - f_1 P \frac{\partial u}{\partial x} - f_2 u \frac{\partial P}{\partial x} - PE - u\sigma, \tag{2}$$

where σ is the relevant stress component. This expansion does not contain anharmonic terms (i.e. the electrostriction term is omitted). When non-linear effects are of interest, these can readily be incorporated into the framework, as done for example in refs. [17–19]. We note in particular that electrostrictive coupling terms always allowed by symmetry, and are in fact essential for the description of perovskite ferroelectrics; for these, the linear piezoelectric term $\theta P u$ in Equation 2 has to be substituted by the electrostrictive coupling term quP^2 [20].

If we set to zero the coefficients for the gradient-containing terms, the bulk equations of state of the material can be found by a simple minimization of potential density (2) with respect to the polarization and strain. Such minimization leads to the standard linear electromechanical equations of a piezoelectric:

$$P = \chi E + eu \tag{3}$$

$$\sigma = eE + cu \tag{4}$$

where $e = \chi\vartheta$ is the so-called strain-charge piezoelectric coefficient. From this we see that the term ϑPu of expansion (2) controls the bulk piezoelectric response. We will drop this term in the further discussion so as to see the electromechanical consequences of pure flexoelectricity without piezoelectricity. However, this discussion can be readily generalized to piezoelectrics by taking this term into account.

Thus, we address flexoelectricity using the thermodynamic potential density (2) with $\vartheta = 0$. Here it is convenient to present Φ_G as the sum of two contributions:

$$\Phi_G = \Phi - \frac{f_1 + f_2}{2}\frac{\partial(uP)}{\partial x} \tag{5}$$

$$\Phi = \frac{1}{2\chi}P^2 + \frac{c}{2}u^2 - \frac{f}{2}(P\frac{\partial u}{\partial x} - u\frac{\partial P}{\partial x}) - PE - u\sigma. \tag{6}$$

where $f = f_1 - f_2$ is the *flexocoupling coefficient* (a tensor in the general case).

Now that the potential density contains gradient terms, to get the equation of state, one should minimize the thermodynamic potential of the sample as a whole $\int \Phi_G dV$ (integrating over the volume of the sample), i.e. to apply the Euler equations $\partial\Phi_G/\partial A - \frac{d}{dx}(\partial\Phi_G/\partial(\partial A/\partial x)) = 0$, where A stands for the variables of the problem (in this case P and u). Such minimization yields the bulk constitutive electromechanical equations in the form:

$$P = \chi E + \mu\frac{\partial u}{\partial x} \tag{7}$$

$$\sigma = cu + \frac{\mu}{\chi}\frac{\partial P}{\partial x}. \tag{8}$$

$$\mu = \chi f. \tag{9}$$

In Equation 7, the first rhs term describes the dielectric response with the clamped dielectric susceptibility χ and the second — the flexoelectric response with the flexoelectric coefficient μ. In Equation 8, the first rhs term describes Hook's law with the elastic constant at fixed polarization c and the second — the converse flexoelectric response. The latter has the physical meaning of a linear response of stress (or strain) to a polarization gradient in a mechanically free sample and was studied by Mindlin [21] and others within the mechanics of materials community, where the theory of (converse) flexoelectricity appears to have developed independently from that of the condensed matter physics community outlined here (for details see Ref. 11).

As is clear from Equation 7, the vector $f\frac{\partial u}{\partial x}$ (or $f_{ijkl}\frac{\partial u_{ij}}{\partial x_l}$ in full tensor notation) has the same effect on polarization as the external electric field E. It is sometimes called the "flexoelectric field" and is a convenient concept when considering the strength of flexoelectric poling effects. For example, when discussing polarization switching or poling caused by strain gradients [22–25], it is this quantity that should be compared with the coercive or built-in electric fields.

It is worth mentioning that the last term in Equation 5 does not contribute to the bulk constitutive electromechanical equations. This can be concluded directly from the fact that its contribution to the thermodynamic potential of the sample can be transformed to an integral over the surface of the sample: $-\frac{1}{2}(f_1 + f_2)\int uPdS$. Thus, the thermodynamic potential density (6) provides a full phenomenological description of the static bulk flexoelectric effect.

The bulk flexoelectric effect describes a strain-gradient-induced polarization

analogous to the strain-induced polarization of the piezoelectric effect. The constitutive Equations 7–9 also highlight an important feature of the bulk flexoelectric effect: Equation 9 explicitly shows that the bulk flexoelectric coefficient μ is proportional to the dielectric permittivity of the material, suggesting that the flexoelectric response should be enhanced in materials with high dielectric constants (high-K materials) such as ferroelectrics.

2.1.2 Direct and Converse Flexoelectricity It is instructive to rewrite the constitutive equations by taking into account that the flexoelectric effect is relatively weak so that P in Equation 8 can be replaced with χE. This gives a set of constitutive equations,

$$\begin{aligned} P &= \chi E + \mu \tfrac{\partial u}{\partial x} \\ \sigma &= \mu \tfrac{\partial E}{\partial x} + cu \end{aligned}, \tag{10}$$

suitable for comparison with the those for the piezoelectric response, which for our one-component 1D model are given by Equations 3 and 4. It is seen that, although for both effects the direct and converse responses are controlled by exactly the same coefficient, there exists a strong asymmetry between the converse and direct flexoelectric effects. Specifically, for the direct effect, in the absence of an electric field, a strain gradient induces a homogeneous polarization. However, for the converse effect, in a mechanically free sample, a homogeneous electric field does not cause a linear deformation (of course, non-linear deformations such as electrostriction still exist). This is in strong contrast to the "symmetric" piezoelectric effect, where strain induces polarization and electric field induces stress as is clear from Equations 3 and 4.

As pointed out in the introduction, however, flexoelectricity is a subtle phenomenon and the aforementioned asymmetry of the bulk flexoelectric effect does

not lead to an asymmetry of the linear electro-mechanical response of a sample as a whole. As a matter of fact, an homogeneous electric field does cause an inhomogeneous deformation for finite size samples, as shall be discussed in section 3.2).

2.2 Dynamic response

The dynamic bulk flexoelectric response can be described by minimizing the action $\int\int(T-\Phi)dVdt$ (the integral being taken over the volume of the sample and time). Here Φ comes from Equation 6 and the kinetic energy density is defined as [16]

$$T = \frac{\rho}{2}\dot{U}^2 + M\dot{U}\dot{P} \tag{11}$$

where ρ and U stand for the density and the acoustic displacement (in the one-dimensional model $u = \partial U/\partial x$); the dot refers to the time derivative. Such minimization with respect to polarization and strain leads to equations of motion for these variables:

$$P = \chi E + \mu\frac{\partial u}{\partial x} - \chi M\,\ddot{U} \tag{12}$$

$$\rho\,\ddot{U} = c\frac{\partial u}{\partial x} - M\ddot{P} + \frac{\mu}{\chi}\frac{\partial^2 P}{\partial x^2}. \tag{13}$$

In Equation 13, the last two terms play an essential role in the lattice dynamics, controlling, for example, the specific shape of the dispersion curve for acoustic phonons in perovskite ferroelectrics [26]. However, for "macroscopic" situations, where the typical spatial scales are much larger than the lattice constant these terms can be neglected. Then, eliminating $\ddot{U}$ from the set of Equations 12 and 13 we get the following equation for the polarization accompanying the strain gradient in a moving medium (e.g. in the case of an acoustic wave)

$$P = \chi E + (\mu + \mu_d)\frac{\partial u}{\partial x} \tag{14}$$

where

$$\mu_d = -\chi c M/\rho \tag{15}$$

is the coefficient describing the dynamic flexoelectric response. The physical meaning of the dynamic flexoelectric effect is clear from Equation 12: it is the polarization induced by the acceleration of the medium. It can be shown that on the microscopic level it can be related to the mass difference of the ions constituting the material [2, 16].

The M coefficient can be calculated in terms of the dynamic lattice theory [16]. **Figure 2** illustrates the static and dynamic contributions to the polarization in an acoustic wave. As is clear form Equation 15, the dynamic contribution scales as the bulk dielectric constant of the material, just like the static one. Of key importance is that these contributions are expected to be of the same order of magnitude, according to estimates [16]. The dynamic contribution to the flexoelectric effect makes it qualitatively different from the piezoelectric effect. For the latter, the polarization and strain in a moving medium are linked by the same relations as in the static case, i.e. $P = \chi E + eu$.

One should mention that the treatment of the dynamic flexoelectric effect in terms of our 1D model is oversimplified. It gives a qualitatively correct picture of the flexoelectric effect in a sound wave where the amplitude of the polarization in the wave is controlled by the sum of static and dynamic contributions. (Remarkably, the relation between these contributions is independent of the frequency of the wave!) However, the typical situation where the time-dependent strain gradient is created by an external mechanical perturbation, is at least two dimensional. In this case, the set of tensor equations corresponding to Equations 12 and 13 does not, in general, yield a relationship like (14). Here, an additional treatment

is needed to evaluate the contribution of the dynamic flexoelectricity to the total polarization response. It can then be shown that it can be neglected in the quasi-static regime, i.e. where the smallest dimension of the sample is less than the acoustic wavelength corresponding to the frequency of the external perturbation. The treatment of this effect is formally similar to that of the piezoelectric resonance in a finite sample.

The framework formulated above for the one-dimensional model can be readily generalized to the real three-dimensional situation. Now the coefficients f, μ, and μ_d become 4th rank tensors symmetric with respect to the permutation of the first pair of suffixes. As being of even rank, these tensors can be non-zero in materials of any symmetry, including amorphous substances. The number of their independent components is controlled by the symmetry of the material (see, e.g., Refs. 27–29). For example, this number is 2 for isotropic materials and 3 for non-piezoelectric cubic materials. Since these tensors do not exhibit any permutation symmetry with respect to the second pair of suffixes, the two-suffix Voigt notations cannot be consistently introduced. Nevertheless, such two-suffix representation (e.g., $\mu_{11} \equiv \mu_{1111}$) will be used in this article, as is customarily done in papers on flexoelectricity.

3 Flexoelectricity in finite samples

Real samples are always finite and thus a complete phenomenological description must include the effects of surfaces or interfaces. In this section we briefly discuss two effects associated with the finite size of a real sample. Although our discussion will explicitly focus on the model system of a cylindrically bent capacitor, the results derived here have profound implications for all finite flexoelectric sys-

tems including thin films and nanodevices that will be discussed in the following sections.

3.1 Contribution of surface piezoelectricity

In a finite sample there will always be surface contributions to any effect. Typically, these are small, being controlled by the surface/volume ratio, but in some cases they can compete with the bulk contribution of another, weaker effect. For example, in centrosymmetric materials, due to the symmetry-breaking impact of the surface, a thin surface layer of thickness λ becomes piezoelectric and can mimic the bulk flexoelectric response. Let us discuss this effect by considering the cylindrical bending of the thin parallel-plate capacitor sketched in **Figure 3**. The piezoelectric coefficients of the surface layers e on the opposite sides of the plate should be of opposite signs (as controlled by the opposite orientation of the surface normal); the same is valid for the bending-induced strains in these layers and, therefore, the induced polarizations in these layers are of the same sign.

The normal component of the electric displacement $D = \epsilon_0 E + P$ across any dielectric interface must be preserved, i.e. $D_z = P_\lambda + \epsilon_0 E_\lambda = P_f + \epsilon_f E_f$. Thus the presence of a polarization P_λ within the piezoelectric surface layers must give rise to internal electric fields in the sample, thus polarising it. For a short-circuited capacitor, the potential difference $\Delta\phi = 2\lambda E_\lambda + hE_f$ across the capacitor must vanish. The electric displacement induced by the strain gradient can then be calculated as [30]

$$D = e\lambda \frac{h\varepsilon_f}{2\lambda\varepsilon_f + h\varepsilon_\lambda} \frac{\partial u_{11}}{\partial x_3}, \tag{16}$$

where $\varepsilon_\lambda = \varepsilon_0 + \chi_\lambda$ is the dielectric constant of the surface layer and ϵ_f is that of the bulk. For thin enough surface layers ($\lambda/h << \varepsilon_\lambda/\varepsilon_f$), Equation 16 yields

the effective flexoelectric coefficient associated with the surface piezoelectricity:

$$\mu_{1133}^{\text{eff}} = e\lambda\frac{\varepsilon_f}{\varepsilon_\lambda}. \tag{17}$$

Thus the polarization of the system arising from surface piezoelectricity is sensitive to the bulk value of the dielectric constant and, for thin enough surfaces layers, is independent of the surface/volume ratio.

Finally, to evaluate the size of this surface effect, let us get an estimate for the effective flexocoupling coefficient $f^{\text{eff}} \equiv \mu^{\text{eff}}/\chi_f \approx e\lambda/\varepsilon_\lambda$. For a conservative lower-bound estimate, we consider the surface layer to be atomically thin ($\lambda =$ 0.4 nm). Then using $e = 1$ C/m^2 and $\varepsilon_\lambda/\varepsilon_0 = 10$, we find $f^{\text{eff}} \simeq 4$ V. This value is about the typical value of the components of the flexocoupling tensor f_{ijkl} ∼1–10 V (see section 4). Thus, we see that the surface piezoelectricity can readily compete with bulk flexoelectricity.

3.2 Polarization-induced bending

As was mentioned in section 2, the electromechanical constitutive equations (10), describing the bulk flexoelectric effect suggest an asymmetry between the direct and converse flexoelectric responses. Specifically, in the absence of electric field, a strain gradient induces a homogeneous polarization while a homogeneous electric field does not induce a strain gradient. It was thus argued that, in contrast to devices based on piezoelectricity, a sensor based on the flexoelectric effect will not behave as an actuator [10]. Meanwhile, a thermodynamic analysis by Bursian and Trunov [31] shows that this is not the case and that a plate of centrosymmetric material should bend under the action of the field due to the flexoelectric coupling, as experimentally observed in barium titanate platelets in both paraelectric and ferroelectric phases [1].

The reason for this discrepancy is that the polarization-induced bending predicted by Bursian and Trunov is a non-local effect that can only be obtained by considering the thermodynamics of the finite-size sample as a whole, and thus is not captured by the "local" theory developed in section 2.1. The finite size of the sample plays a critical role because the strain energy of a bent plate increases with the cube of its thickness and thus the bending can only be observed in sufficiently thin samples.

The origin of the polarization-induced bending moment can actually be understood by considering what happens at the sample surface. If the polarization at the surface of the plate changes continuously from its bulk value P to zero outside the plate, then, according to Equation 8, the polarization gradients at plate surfaces must create some stress via the converse flexoelectric effect, resulting in forces applied to the opposite surfaces of the plate [30, 32]. The mechanical moment of these forces causes the bending predicted by the Bursian-Trunov approach. It can thus be shown that a bending-mode flexoelectric sensor working as an actuator will, in fact, be characterized by the same effective piezoelectric constant [30].

For more general boundary conditions the situation is more complex and requires the use of modified mechanical boundary conditions [30,33]. Failure to take into account these flexoelectricity-induced modification of mechanical boundary conditions can lead to explicit conflicts with thermodynamics (see, e.g., Ref. 32).

4 Microscopic calculations of bulk flexoelectricity

So far, we have not actually addressed the magnitude of the flexoelectric effect. A rough, order of magnitude, theoretical estimates of the flexocoupling coefficient

was first given by Kogan [15]. Subsequently, other approaches were shown to lead to essentially the same result [2, 34] The most straightforward way to arrive at Kogan's estimate is to consider a simple lattice of point charges q with interatomic spacing a. Let this lattice be distorted by an "atomic scale" strain gradient of order $1/a$ and with an "atomic scale" polarization of the order of $(ea)/a^3$. Such a strong perturbation is expected to modify the energy density in the material, which is of the order of $\sim \frac{q^2}{4\pi\epsilon_0 a}\frac{1}{a^3}$, by a comparable amount. Assigning this energy change to the flexoelectric term $fP\frac{\partial u}{\partial x}$, yields Kogan's estimate of the flexocoupling coefficient

$$f \approx q/(4\pi\epsilon_0 a) \sim 10 \text{ V}, \tag{18}$$

using the electronic charge for q and a of the order of an Ångstrom.

Since Kogan's seminal work of 1964, there have been a number of attempts to properly quantify the flexoelectric response in solids. On the microscopic level, static bulk flexoelectricity can be viewed as strain-gradient-driven charge redistribution in the material. Roughly speaking, one can distinguish two contributions to this redistribution: ionic and electronic. The first attempts to quantify the ionic contribution were undertaken by Askar *et al.* who used a shell model for the lattice dynamics of ionic crystals to calculate a full set of flexocoupling coefficients for a number of bi-atomic cubic crystals [35]. A microscopic theory of ionic flexoelectricity based on a rigid-ion model was then developed by Tagantsev in the late 1980's [4, 16]. The first steps towards a microscopic description of the electronic contribution to flexoelectricity [36, 37] were recently made by generalizing the Martin's approach [38] to piezoelectricity.

To gain some microscopic understanding of the ionic contribution to flexoelectricity, let us begin by briefly discussing the theory developed by Tagantsev.

When a crystalline lattice is deformed, the displacement along i of the nth atom, $w_{n,i}$, can be expressed as a sum of two terms:

$$w_{n,i} = \int_{x_j^0}^{R_j^n} \frac{\partial U_i}{\partial x_j} dy_j + w_{n,i}^{\text{int}} \tag{19}$$

where x_j^0 and R_j^n are the coordinates of an immobile reference point and that of the n^{th} atom before the deformation, and summation over the three Cartesian coordinates is assumed for all repeating suffixes. The first rhs term in Equation 19 represents the contribution of the unsymmetrized strain $\partial U_i/\partial x_j$ taken in the elastic medium approximation, also known as external strain. It the case of homogenous strain it has a simple meaning: the displacement of each atom is proportional to the distance to it from a certain immobile point. For a material where all atoms are centers of inversion, the external strain is sufficient to describe all atomic displacements caused by a homogeneous deformation. Consider, for instance, the simple centrosymmetric atomic lattice sketched in Figure 4a with $c = 2a$. Under the homogeneous deformation shown in Figure 4b, centrosymmetry is preserved ($\delta c = 2\delta a$) and the displacements of the white and black atoms follow the external strain field, which is represented by the deformation of the blue lattice.

However, if the material is noncentrosymmetric or if the deformation is inhomogeneous, the white and black atoms are no longer constrained by symmetry and may undergo additional internal displacements within the deformed unit cell. These internal displacements—the difference between the real displacement of an atom and that calculated from the local external strain—are known as internal strains [39] and are described by the second rhs term in Equation 19. Figure 4c shows the same centrosymmetric atomic lattice stretched inhomogeneously along x_1. The longitudinal strain gradient breaks the centrosymmetry and thus the

displacements of (in this case) black atoms no longer have to follow the external strain field (the blue lattice).

For a piezoelectric (noncentrosymmetric) material, the internal strains are responsible for the change in polarization under homogeneous strain and are, to lowest order, proportional to the macroscopic strain $u_{ij} = (\partial U_i/\partial x_j + \partial U_j/\partial x_i)/2$. For a centrosymmetric material, the internal strain of the n-th atom is, to lowest order, proportional to the elastic gradient:

$$w_{n,j}^{\text{int}} = w_{n,j}^{\text{flex}} \equiv N_{n,j}^{ikl} \frac{\partial u_{ik}}{\partial x_l}. \tag{20}$$

If the body is considered to be made up of point charges Q_n (this includes all charges, not only ions) with the coordinates $R_{n,i}$, the response of the polarization to an inhomogeneous deformation can be found by calculating the variation of the average dipole-moment density caused by this perturbation

$$\delta P_i = V_{\text{fin}}^{-1} \sum_n Q_n (R_{n,i} + w_{n,i}) - V^{-1} \sum_n Q_n R_{n,i} \tag{21}$$

where V and V_{fin} are the sample volume before and after the deformation. Substituting Equation 19 into 21 one finds several contributions to the induced polarization (for details of the full expansion the reader is referred to Refs. 16 and 4). Among these is a term proportional to strain, which is non-zero only in the case of noncentrosymmetric materials and describes the bulk piezoelectric response. In addition, there are two terms proportional to the strain gradient. The first of these describes the bulk flexoelectric effect with a flexoelectric coefficient given by

$$\mu_{ikjl} = v^{-1} \sum_n Q_n N_{n,j}^{ikl}, \tag{22}$$

where the summation is taken over the ions in a unit cell of volume v. The second term is termination dependent and describes the surface flexoelectric effect. The

existence of this effect was recently questioned by Resta [36]. [1] Its contribution, however, is not expected to be enhanced in high-K materials and is therefore of minor importance for applications; we will therefore exclude it from further consideration.

The tensor $N_{n,j}^{ikl}$ above, which links the internal strains and strain gradients, can be calculated from the dynamic matrix of the material [16], which in turn can be obtained from *ab initio* lattice dynamics simulations. Using this tensor and the transverse Born ionic charges (obtained, e.g., from Berry-phase calculations) one can obtain the μ-tensor using Equation 22. This approach was implemented by Pradeep Sharma and co-workers from the University of Texas to calculate the flexoelectric coefficients for a number of materials (see Ref. 40 and **Table 2**).

An alternative way to obtain the μ-tensor consists of direct calculations of the polarization response in an inhomogeneously deformed crystalline lattice. In view of the periodic boundary conditions typically required for first principles calculations, consideration of a periodic distribution of the strain gradient (as the source of a "static" wave of internal strains) is a reasonable option. Then once the transverse Born ionic charges are available, the amplitude of the polarization wave can be found. This approach was directly implemented by Hong *et al.* [41] in their calculations for some ferroelectric perovskites (see **Table 2**). These authors introduce the static strain wave via fixing the positions of the A-site atoms as sinusoidal function of the distance, the direction of the atomic displacements and the modulation direction being parallel to a cubic crystallographic axis, so that the flexoelectric response related to the μ_{11} component of the flexoelectric

[1] This paper also claims that the dynamic contribution to the flexoelectric effect (see section 2.2) does not exist either.

tensor was simulated. One drawback of this approach is that such a simulation does not provide all the information needed to evaluate this component in view of the depolarizing-field problem. Specifically, such conditions of the simulation imply conservation of the longitudinal component of electrical displacement and the effective coefficient μ_D extracted from such a simulation is related to the true coefficient μ via $\mu_D = \mu/(1 + \chi/\varepsilon_0)$. Thus, in the case of high-K materials (like ferroelectric perovskites) with $\chi >> \varepsilon_0$, the calculated μ_D does not yield μ whereas μ_D/ε_0 appears to be close to the flexocoupling coefficient $f = \mu/\chi$. In order to calculate the μ coefficient within this framework, additional simulations of χ are required.

The depolarizing-field problem was circumvented in finite-temperature simulations of μ and f tensors by Ponomareva *et al.* [42]. Here the effect was addressed by employing Monte Carlo simulations with an *ab initio*-calculated effective Hamiltonian; the contribution of the depolarizing energy was deliberately eliminated. A drawback of this work is that, in the *ab initio* calculations of f tensors (used also in the Monte Carlo simulations of μ), only the interaction between the local dipole and strain inside one unit cell was taken into account, and such approximation can readily entail some 50% inaccuracy.

A disadvantage of the three aforementioned methods is that the purely electronic contribution (or "frozen-in" contribution [37]) to bulk flexoelectricity is missing from these. This is probably a minor drawback when it comes to high-K materials where it is the ionic contribution that is enhanced and dominates the total μ-tensor, but clearly a complete theory should incorporate the electronic contributions also. The first principles calculations of the purely electronic contribution to bulk flexoelectricity have been done by Hong and Vanderbilt [37].

The concept behind these calculations, stemming form the classical work by Martin [38], was formulated by Resta [36]. Here the so-called frozen-in contribution was evaluated by calculating the response of the polarization to lattice distortions with strain gradients in the "elasticity-theory approximation" (no internal strains).

One should mention that these calculations were also performed under conditions of fixed electrical displacement so that the evaluated "electronic" flexoelectric coefficient is underestimated by a factor of $(1 + \chi_{\mathrm{el}}/\epsilon_0)$. First principles calculations of the purely electronic contribution to the total flexoelectric response (including possible surface conditioned contributions) were also performed by Dumitrica et al [43] and Kalinin and Meunier [5] for carbon systems.

5 Experimental studies of flexoelectricity

5.1 Quantifying flexoelectricity in bulk

The static flexoelectric response is most commonly measured using some variation of the two methods sketched in **Figure 5**. The first method consists of dynamically bending the material in a cantilever beam geometry in order to generate a transverse strain gradient, as shown in **Figure 5a**. The flexoelectric polarisation can then be measured by recording the displacement current flowing between the metallic plates with a lock-in amplifier. In this way the coefficient $\tilde{\mu}_{12}$ where

$$P_3 = \tilde{\mu}_{12} \frac{\partial u_{11}}{\partial x_3}$$

can be calculated; here the flexoelectric tensor is expressed using the two-suffix notation. The cantilever bending method has been used extensively to investigate flexoelectricity (also referred to as "bending piezoelectricity") in polymers [44–46]

and was recently used by Ma and Cross to systematically quantify the flexoelectric response in a number of perovskite ceramics [47–51]. Variations of the method involving three- or four-point bending geometries have also been successfully employed [10, 52, 53]. A point to remember is that the cross section of a bent beam is modified due to anticlastic bending (as sketched in **Figure 5a**), giving rise to non-zero u_{22} and u_{33} components and their corresponding gradients, related to u_{11} through the Poisson ratio ν. Thus $\tilde{\mu}_{12}$ is actually an *effective* flexoelectric coefficient involving a combination of flexoelectric tensor components that depends on the precise geometry of the system [53, 54]. In the case of an isotropic bent beam, for example, $\tilde{\mu}_{12} = -\nu\mu_{11} + (1-\nu)\mu_{12}$.

A second method for measuring direct flexoelectricity was developed by Ma and Cross and involves uniaxial compression of a truncated-pyramid-shaped sample [10], as illustrated in **Figure 5b**. The stress $\sigma_{33} = F/A$, generated by the pair of forces F, is different at the top and bottom surfaces of the truncated pyramid due to their different areas A, setting up a longitudinal strain gradient and thus generating a flexoelectric polarisation $P_3 = \tilde{\mu}_{11}\frac{\partial u_{11}}{\partial x_3}$. Again, $\tilde{\mu}_{11}$ is an effective coefficient, which in the case of an isotropic material is related to the flexoelectric tensor components through $\tilde{\mu}_{11} = \mu_{11} - 2\nu\mu_{12}$. In practice, the pyramid-compression approach is complicated by the fact that the strain gradient is strongly inhomogeneous [55] (concentrated mainly at the sample edges) making it difficult to extract reliable values of $\tilde{\mu}$.

Conversely, application of a bias across such a structure gives rise to a non-uniform field distribution and hence polarization gradients that, in turn, generate strain in the sample through the converse flexoelectric effect, which can be measured using interferometric techniques [10,56]. Such measurements always include

contributions from electrostriction, which usually dominate the signal. However, the field dependence is different for electrostriction (quadratic) and flexoelectricity (linear) and therefore the two effects can, in principle, be separated. This method was used by Fu and coworkers to measure the converse flexoelectric effect and thus estimate the flexoelectric coefficient $\tilde{\mu}_{11}$ for BST, which was found to be in excellent agreement with measurements of the direct flexoelectric effect [56]. A similar method was also used by Hana *et al.* to study converse flexoelectricity in PMNPT [57, 58].

Extracting the full flexoelectric tensor is nevertheless challenging even for the simplest cubic dielectrics with only three independent coefficients. Zubko *et al.* employed a dynamical mechanical analyser in the three-point bending configuration to generate flexoelectric polarisation in non-piezoelectric $SrTiO_3$ single crystals of different crystallographic orientations. However, pure bending experiments yield only two independent equations for the three flexoelectric tensor components and thus must be combined with a different method to obtain all three tensor components [54].

One possibility would be to use the pyramid-compression method illustrated in **Figure 5b**. Another, less direct, method involves accurate measurements of transverse optical phonon frequencies, which are renormalized by the flexoelectric terms and thus can be used quantify the flexoelectric coefficients [17]. This method, however, will generally give the sum of the static and dynamic responses.

The flexoelectric coefficients for a number of perovskite ceramics are listed in **Table 1**. Particularly high flexoelectric coefficients (tens of μC/m and more) have been measured close to the ferroelectric-to-paraelectric phase transitions of (Ba,Sr)TiO_3, relaxor PMN and (Pb,Sr)TiO_3 ceramics, where the dielectric

constants reach values exceeding 10000–20000. Measurements of the flexoelectric response as a function of temperature confirm the expected scaling of μ with χ, as illustrated in **Figure 6** for several perovskite compounds in their paraelectric phases. The exact proportionality between μ and χ predicted by Equation 9, however, does not always hold, as can be seen most clearly in **Figure 6b**. Due to the large differences in dielectric permittivities of different compounds, it is more instructive to compare the normalized (or flexocoupling) coefficients $f = \mu/\chi$ measured in Volts, which were predicted by Kogan to be of the order of $f \approx q/(4\pi\epsilon_0 a) = 1$–$10$ V (Equation 18) for simple ionic solids.

For all the materials listed in **Table 1**, the absolute magnitude of the response greatly exceeds this simple theoretical estimate. $BaTiO_3$-based ceramics, in particular, show enormous flexoelectric and flexocoupling coefficients. Such large flexoelectric coefficients are particularly puzzling as theoretical considerations suggest that flexocoupling coefficients in excess of 10–15 V should make the perovskite structure unstable to formation of incommensurate phases; this will be discussed in more detail in section 5.2.5. For PMN-PT, the measured coefficients were found to vary by orders of magnitude depending on the measurement method used [57, 58].

Experimental data for single crystals are shown in **Table 2** together with theoretical coefficients calculated using density functional theory. Although direct comparison with ceramics is difficult due to the scarcity of single crystal data and the different measurements techniques used in most cases, the flexocoupling coefficients for single crystals are generally found to be considerably lower. For $SrTiO_3$—the only monocrystalline material whose full static flexoelectric tensor has been quantified—the magnitude of the flexoelectric response is in good

agreement with Kogan's estimate [53,54] (although there is still some uncertainty about their signs). Neutron and Brillouin scattering measurements on $BaTiO_3$ and $KTaO_3$ single crystals give values of the same order of magnitude. [26,59–61] It should be noted, however, that all of the values given in **Tables 1** and **2** should be treated as order of magnitude estimates only. Challenges to properly quantifying flexoelectricity arise from difficulties in separating the bulk flexoelectric response from surface piezo- and flexoelectric contributions as well as dynamic flexoelectricity. It has been generally assumed that in high-K dielectrics, the contributions from surface piezoelectricity should not be significant, as they were not expected to scale with the bulk dielectric constant of the material. This, however, appears not to be the case, as was discussed in section 3.1 and thus all the experimental bulk static flexoelectric coefficients may well be affected by this contribution. Meanwhile, neutron and Brillouin scattering measurements are affected by the dynamic flexoelectric effect.

We have deliberately excluded polymers and elastomers from **Tables 1 and 2** as the nature of the effect is very different in these materials and is beyond the scope of this review. Nevertheless, it is worth mentioning that the flexibility of these materials makes them in principle attractive candidates for future flexoelectric devices and has motivated many studies on flexoelectricity in polymers. Recently, extremely large flexoelectric coefficients were reported for polyvinylidene flouride (PVDF) thin films by Baskaran *et al.* [55,62,63], but there is still no consensus on the best methods for quantifying flexoelectricity in these materials, leading to very large variations between the values reported for different polymers by different groups [44–46,64,65]. For PVDF alone, the reported coefficients range from 13 nC/m [65] to 80 μC/m and higher [55,62,63].

Quantifying the flexoelectric tensor theoretically has proven to be equally challenging. Nevertheless, a number of different approaches have been developed to calculate the flexoelectric coefficients, as reviewed in section 4. The results of such calculations for a variety of materials are summarized in **Table 2**.

For $SrTiO_3$, the theoretical and experimental values are of the same order of magnitude though there is still significant disagreement (including in the signs) between values obtained using different theoretical methods. For other materials, notably barium titanate, the disagreement between theory and experiment is much larger. In all cases, however, the calculations yield f-values comparable to or smaller than Kogan's estimate (Equation 18) and thus cannot account for the large coefficients measured for ferroelectric ceramics.

In summary: despite significant experimental and theoretical effort, reliable quantification of the flexoelectric response remains challenging. While there is some convergence on the order of magnitude of the response for some monocrystalline oxides, there are still large, unexplained discrepancies between experimental data on ceramics and single crystals, and equally large differences between theoretical values obtained using different techniques. The importance of building an accurate database of flexoelectric tensor components for a wide range of materials should not be overlooked since, as we shall see next, flexoelectric effects are ubiquitous at the nanoscale, and must be properly included for accurate modelling of nanoscale structures and devices.

5.2 Manifestations of the flexoelectric effect in solids

5.2.1 Strain gradients in thin films As we have seen from **Tables 1 & 2**, the largest flexoelectric coefficients have been measured in ferroelectric

materials, which tend to have large dielectric constants. Bearing also in mind that gradients are inversely proportional to size, ferroelectric thin films are thus the obvious place to look for large flexoelectric effects, as they combine small size and big permittivity. Indeed, it is in ferroelectric thin films where some of the most dramatic manifestations of flexoelectricity have been reported.

All thin films are grown on rigid substrates, and stresses normally appear due to the mismatches in lattice parameters and thermal expansion of the film and the substrate. The substrate-induced strain state in the films may be homogeneous if they are sufficiently thin. However, whenever the thickness exceeds some critical value, it is possible for the films to relieve the stress by dislocating from the substrate [66] or by twinning if the film is ferroelastic. Both these relaxation mechanisms are highly inhomogeneous and generate flexoelectric effects.

The effect of strain gradients on the dielectric constant of thin films was studied by Catalan *et al.* [18, 67]. Their assumption, based on earlier work by Kim *et al.* [68], and consistent with X-ray diffraction analysis [67] was that the mismatch strain does not relax suddenly at the surface but exponentially through the film. When the flexoelectricity caused by the exponential strain relaxation is introduced into the free energy of the system, it causes an orders of magnitude decrease in the dielectric constant and complete smearing of the dielectric peak at the ferroelectric Curie temperature. This can be understood by recalling that the effect of the flexoelectricity is analogous to that of applying an external electric field (see section 2.1), and external fields decrease the permittivity by saturating the polarization.

The adverse impact of flexoelectricity on the dielectric constant of thin films has also been analyzed using atomistic calculations by the group of Sharma [69].

These authors showed that the gradient arising from intrinsic surface tension leads to a flexoelectrically-induced lowering of the permittivity that mimics the well known "dead layer effect" [70]. Thus, even for perfectly coherent thin films with well matched electrodes, surface flexoelectricity will still act to prevent the permittivity of the films from being as large as that of bulk samples. Flexoelectricity has also been predicted to increase the critical thickness (or decrease the critical temperature) for ferroelectricity in thin films [71]. Experimentally, the connection between surface gradients and polarization was also pointed out by Scott [72] who showed that surface stresses induced by polishing can cause the appearance of polar modes in otherwise centrosymmetric single crystals. Kholkin *et al.* [73] has also shown that the grain boundaries of polycrystalline $SrTiO_3$ (a centrosymmetric material) have a piezoelectric response consistent with surface-gradient-induced flexoelectricity.

5.2.2 Flexoelectric poling and imprint By analogy with electric fields, strain gradients skew the thermodynamic potential, as illustrated in **Figure 7** and may lead to preferential poling of the material. For example, the poling of quasi-amorphous $BaTiO_3$ upon cooling was reported to be assisted by flexoelectricity by the group of Lubomirsky [74]. In ferroelectrics, strain gradients can lead to imprint—asymmetric polarization-field hysteresis loops. This effect is expected to be particularly appreciable in ferroelectric thin films where the misfit strain due to the underlying substrate is relaxed though formation of dislocations, giving rise to large strain gradients [75]. Experimentally, the effect of strain gradients on polarity has been discussed by several authors [22, 24, 25, 76], and Lee *et al.* in particular directly showed the correlation between asymmetric hysteresis loops (and domain population), and strain gradients, measured using

grazing incidence x-ray diffraction in thin films of $YMnO_3$ (see **Figure 7** and Ref. 24). An extreme manifestation of the effect of flexoelectricity on polarity is the discovery that strain gradients can be used to actively switch the polarization of a ferroelectric [22, 25]. This phenomenon is further discussed in section 6.3.

Note that, although flexoelectricity appears to play an important role in a number of poling phenomena, in many cases [22, 74, 76] the magnitude of the flexoelectric coefficients required to explain the experimental observations purely by flexoelectricity exceeds physically reasonable values by several orders of magnitude, suggesting that other contributions also play a role.

5.2.3 Elasticity and lattice dynamics As we have discussed, both the static and dynamic flexoelectric effects will lead to a modification of the phonon dispersion curves [26]. This effect has been investigated in single crystals of $SrTiO_3$ [77] and $KTaO_3$ and was used to estimate the total (static + dynamic) bulk flexocoupling coefficients for these materials (see **Table 2**).

Flexoelectricity may also affect the elastic properties of materials and thus the measurements of the elastic constants. In particular, the electrostatic cost of generating flexoelectric charge causes a depth-dependent stiffening in nanoindentation experiments, owing to the very inhomogeneous nature of the stress introduced by a nanoindenter. This effect was studied both experimentally and theoretically for several materials by the Texas group [78–80].

5.2.4 Polarization-induced bending During the late 60's and early 70's, Bursian and coworkers studied the phenomenon of polarization-induced bending which we have already touched upon in section 3.2. Arguing that the development of a polarization should lead to an inhomogeneous deformation of the perovskite unit cell, the effect was demonstrated by observing the bending of a 2.5 μm-thick

ferroelectric $BaTiO_3$ plate as its polarization was switched by an applied electric field (**Figure 8a**) [1].

By measuring the curvature ζ induced by the electric field E, one can also get an estimate of the flexoelectric coefficient which is given by

$$\tilde{\mu}_{12} = \frac{\zeta}{E} \cdot \frac{Gd^2}{12(1-\nu)} \tag{23}$$

where G is the Young's modulus, d the crystal thickness and ν the Poisson ratio. From the data of Bursian and Zaikovskii, reproduced in **Figure 8b**, we estimate $\tilde{\mu}_{12}$ to be of the order of 0.1–1 μC/m in the paraelectric phase of $BaTiO_3$, close to the phase transition. Taking the dielectric constant of $BaTiO_3$ to be around 10000 at these temperatures, we obtain a flexocoupling coefficient $\tilde{f}$ ∼1–10 V.

Later, Bursian proposed another manifestation of the converse flexoelectric effect. For regular 180° ferroelectric domain structures, domains of opposite polarization would distort in the opposite sense, leading to no net macroscopic bending of the sample, as sketched in **Figure 8c**. Again, this effect is expected to be most pronounced in thin ferroelectric layers. Superlattices composed of alternating ultrathin ferroelectric and non-ferroelectric layers may thus be an ideal system to observe this phenomenon. Indeed, such inhomogeneous strain distributions have been predicted via DFT calculations of $PbTiO_3/SrTiO_3$ superlattices by Aguado-Puente and Junquera [81]. These considerations imply that, in thin ferroelectrics, there may be a strong elastic component to the formation of 180° domains [82], usually assumed to be dictated only by the electrostatic boundary conditions, and may help explain the large coherence lengths for the domains observed in $PbTiO_3/SrTiO_3$ superlattices [81, 83].

5.2.5 Domain boundary flexoelectricity Interfaces, including surfaces and domain boundaries, can give rise to a multitude of fascinating physical

phenomena that are absent from the bulk of the host materials [84–86]. Recent discoveries of novel functionalities within ferroelectric and ferroelastic domain walls have generated tremendous excitement within the nanoelectronics community [86, 87]. Such domain walls are intrinsically very narrow, and their internal gradients are therefore intrinsically very large, which, in turn, should lead to large flexoelectric and flexomagnetic effects (see special topic box on flexomagnetism). For example, even for $SrTiO_3$, with its very modest tetragonality ($c/a \approx 1.00056$ below 105 K) [88], the strain gradients within the ferroelastic domain walls can reach values of the order of 10^5–10^6 m^{-1} [89], which translates into polarization values of 0.1–1 $\mu C/cm^2$—larger than the spontaneous polarization of many multiferroic ferroelectrics. Detailed phenomenological calculations by Morozovska *et al.*, which take into account the various couplings between polarization, rotations of the TiO_6 octahedra, strain, strain gradients and depolarizing fields in a fully self-consistent manner, yield somewhat lower, but still sizable estimates [19]. As the temperature is reduced below 105 K, the calculated flexoelectric polarization increases to $\sim$0.01 $\mu C/cm^2$ within 90° twin boundaries and to $\sim$0.1 $\mu C/cm^2$ in the anti-phase boundaries of $SrTiO_3$. Moreover, at still lower temperatures ($\sim$50 K for anti-phase boundaries and $\sim$40 K for twin walls), a switchable ferroelectric polarization of several $\mu C/cm^2$ develops due to the biquadratic coupling term $\eta_{ijkl}P_iP_j\Phi_k\Phi_l$, where Φ is the order parameter describing oxygen rotations [17, 19]. The inhomogeneous flexoelectric polarization at such domain walls may help explain the apparent suppression of the flexoelectric response observed in $SrTiO_3$ single crystals below 105 K and attributed to polar or charged domain walls [53]. Polar domain walls were also recently invoked [90] to explain the low temperature elastic anomalies of $SrTiO_3$ [91]. Janovec has

recently remarked that all ferroelastic domain walls must, by symmetry, be polar (private communication).

The recent discovery of phase coexistence in highly strained $BiFeO_3$ thin films offers an exciting opportunity for engineering large strain gradients on the nanometer scale. At the phase boundary between the "tetragonal-like" T-phase and "rhombohedral-like" R-phase, the out-of-plane lattice parameter changes from ~ 4.1 Å to ~ 4.6 Å over a distance of ~ 10 perovskite unit cells (~ 40 Å) [92], giving rise to a local strain gradient in excess of 10^7 m^{-1} [93]. Interestingly, in addition to large flexoelectric effects, one may also expect significant flexomagnetic effects (see special topic box on flexomagnetism and Ref. 94) in this system as bulk $BiFeO_3$ is both ferroelectric and antiferromagnetic at room temperature. Zhang *et al.* have proposed that such flexomagnetic effects at phase boundaries may be responsible for the enhanced magnetism observed in their mixed phase $BiFeO_3$ films [93].

Flexoelectricity can also have dramatic consequences for the conductivity of domain walls—a topic which is currently generating an enormous amount of interest within the ferroelectrics community [86, 95]. Even in the nominally uncharged 180° ferroelectric domain walls, the flexoelectric effect can lead to the development of inhomogeneous polarization perpendicular to the domain wall. This gives rise to an internal depolarizing field that leads to a redistribution of the free carriers within the semiconducting material and either accumulation or depletion of carriers around domain walls [96, 97].

Within the Landau-Ginzburg-Devonshire formalism, the description of domain walls involves the inclusion of the gradient term $\frac{g}{2}\left(\frac{\partial P}{\partial x}\right)^2$ in the free energy expansion (Equation 6), where g determines the domain wall energy. The effect of

the flexoelectric coupling is to renormalize this gradient coefficient $g \to g - f^2 s$, where s is the elastic compliance [17, 18, 32]. Hence, if f is large enough, the domain wall energy can become negative, making the material unstable with respect to the development of modulated phases. Borisevich *et al.* argued that this is precisely what happens at the ferroelectric-antiferroelectrics phase boundary in Sm-substituted $BiFeO_3$ thin films [98]. In terms of lattice dynamics theory, the instability arises from the interaction (or "mode coupling") between the optical and acoustic phonons, as originally discussed by Axe *et al.* [26]. For large enough flexoelectric couplings, the optical branch pushes the acoustic one to zero frequency at a certain point with $q \neq 0$ in the Brillouin zone, leading to an incommensurate phase.

Just like within ferroelastic domain walls, strain gradients are also very large around dislocations and thus are expected to give rise to large local flexoelectric polarizations. Nanoscale gradients were also proposed to play a role in the appearance of polarization in relaxors [99].

6 Toward applications of flexoelectricity

6.1 Piezoelectric meta-materials and nanodevices

The revival of flexoelectricity can in part be attributed to the realization of Fousek, Cross and Litvin [100] that a nanocomposite with built-in shape gradients can produce an effective piezoelectric response irrespective of whether its constituents are piezoelectric or not. Flexoelectricity can thus be turned from a nuisance to a useful functional property, opening the applications of piezoelectricity to a whole new class of materials. In 2007, Cross and coworkers filed a patent for a simple device illustrated in **Figure 9a** [10, 100, 101]. It consists of an array

of truncated dielectric pyramids with a high flexoelectric coefficient, like those discussed in section 5.1, embedded in another medium (which could simply be air) and sandwiched between two metallic plates. When the plates are compressed, a stress gradient is generated in each pyramid, inducing a flexoelectric polarization and thus an effective piezoelectric response. Devices with dimensions in the 10–100 μm range have been fabricated using BST as the dielectric, and effective piezoelectric coefficients up to ~ 40 pC/N have been demonstrated, along with the expected scaling with size [101,102]. A similar type of meta-material was studied theoretically in the group of P. Sharma [103]. They considered a non-piezoelectric elastic matrix with nanoscale inhomogeneities (nano-inclusions) which lead to local strain gradients. To achieve an effective macroscopic piezoelectric effect, the shape and distribution of such inhomogeneities must be non-centrosymmetric to avoid cancellation of local flexoelectric moments. Recently, the group proposed that even graphene could in principle be made piezoelectric by breaking the centrosymmetry of the hexagonal lattice with nanoscale holes [104].

A piezoelectric composite based on the transverse, rather than longitudinal, flexoelectric effect is sketched in **Figure 9b** [105]. The charge generated by bending the flexoelectric material is collected by metallic strips located at positions where the strain gradient is maximum. Effective piezoelectric coefficients of several thousand pC/N, were reported. Although care must be taken when comparing the effective piezoelectric coefficients of such bending-mode composites with those of standard bulk piezoelectrics measured under compression, these results are very promising for future applications of flexoelectric composites.

The expected enhancement of flexoelectricity at the nanoscale has also stimulated theoretical work on piezoelectric nanodevices. The group of Sharma has

led the field with atomistic calculations on various types of nanostructures, including nano-cantilevers, nano-composites and superlattices. For example, they have shown that flexoelectric effects could as much as double the energy harvesting potential of piezoelectric PZT cantilevers if their thickness could be reduced down to ~ 20 nm [106].

The last decade has seen some tremendous advances in the fabrication and characterization of oxide nanocomposites. The regular arrays of dielectric nanopyramids envisaged by Cross *et al.* have, in effect, been realized by a number of groups [107,108], as have nano-cantilevers [109], tri-color superlattices [110], buckled nano-ribbons [111], nano-tubes and other nano-shapes and nano-composites where large flexoelectric effects could be observed. The effects of flexoelectricity, however, have rarely been considered when characterizing such structures [112] and thus the predicted flexoelectric effects discussed above remain to be tested experimentally.

6.2 Strain gradient engineering

The use of epitaxial strain to modify the properties of thin films is a mature area of research [113], and strain engineering has some impressive achievements to show, from doubling the critical temperature of some superconductors [114] to turning $SrTiO_3$ into a room temperature ferroelectric [115]. There has been much less work on strain *gradient* engineering, but the growing awareness of flexoelectricity is starting to change this.

An idea proposed by Sharma *et al.* relies on strain gradients at surfaces or interfaces between different non-piezoelectric materials [116]. Compositionally graded superlattices are in fact an older concept [117], so it is surprising that the

flexoelectric contribution to their performance had not been considered until now. Strain gradients should give rise to an interfacial flexoelectric dipole, rendering the material piezoelectric. In a superlattice configuration, such dipoles would point in opposite directions at neighboring interfaces, leading to a cancellation of the piezoelectric response. To achieve macroscopic piezoelectricity, the inversion symmetry must be broken, for example by adding a third component layer to form so-called tri-color superlattices [118], as illustrated in **Figure 9c**, or by having a net compositional gradient between the top and bottom layer of the film.

A different type of gradient can be engineered by growing films with ferroelastic twins (domains with alternate directions of spontaneous deformation). Twinning is a well known strain relaxation mechanism in thin films, where the orientation and size of the twins can be controlled with the substrate mismatch and film thickness [119, 120]. Catalan *et al.* have noticed that the nanotwins that appear in a clamped film generate strong lateral strain gradients with associated flexoelectric polarizations of the order of μC/cm^2, comparable to the size of spontaneous ferroelectric polarization in standard perovskite ferroelectrics (see **Figure 10**). This lateral flexoelectricity combines with the vertical ferroelectricity to yield a tilted polar vector [121]. The hope is now that, as in morphotropic phase boundary piezoelectrics, the tilted polarization of twinned films will also result in enhanced piezoelectricity.

6.3 Mechanical polarization switching

Properly harnessed, flexoelectricity enables a control of polarity its effect is equivalent to that of an external electric field, as explained earlier. In 1969, Bursian

and coworkers discussed the possibility of ferroelectric switching driven by a strain gradient and showed that the bending of a few-micron-thick plate of $BaTiO_3$ can result in the reversal of the sign of its pyroelectric coefficient [76]. The active control of polarity by strain gradients in thin films was reported by Gruverman *et al.*, who demonstrated that the polarization state of a ferroelectric $Pb(Zr,Ti)O_3$ capacitor can be reversed by strain gradients generated by bending of the underlying Si substrate [22]. Recently, Lu *et al.* [25] used the inhomogenous deformation caused by pushing with the tip of an atomic force microscope in order to switch the polarization of an ultrathin $BaTiO_3$ film (see **Figure 11**). As the authors argue, the conversion of mechanical pressure into readable information is conceptually analogous to the functioning of a nanoscopic typewriter. The flexoelectric switching of polarization has a useful advantage in that it removes the need for large (coercive) electric fields and thus associated problems such as leakage or breakdown.

Though most of our discussion has focused on ferroelectric materials, which tend to display the largest flexoelectric coefficients, flexoelectricity is also highly relevant to other systems such as ionic conductors. Morozovska *et al.* have shown, for example, that flexoelectric effects should play an important role in the electrotechnical properties of Li-battery materials [122].

7 Unresolved issues and future trends

As Niels Bohr famously said, "prediction is very difficult, especially about the future". Anticipating the future research in any field is a tricky and somewhat futile exercise, but there are obvious gaps that need to be filled, and this is a good indicator of where research may be or should be concentrating.

At the time of writing, there is not yet a universal consensus regarding the size, or even the sign, of the flexoelectric tensor components for any material. For the best studied one, $SrTiO_3$, there is some convergence regarding the order of magnitude of the coefficients with experimental values being consistent Kogan's estimate and some theoretical models. The sign of the coefficients, however, has not yet been settled, and there is still a significant variation in the values predicted by different models. For other systems, such as $BaTiO_3$, the situation is even worse: experimentally, only effective coefficients are available and the calculations and the measurements disagree by several orders of magnitude [41]. Solving the reason for these discrepancies, and finding reliable methods for measuring flexoelectricity, should be a priority both for experimentalists and theoreticians alike. We need to build a robust catalogue of flexoelectric coefficients for all materials of technological interest, so that flexoelectricity can be reliably incorporated into the calculations of performance at the nanoscale. The best flexoelectrics may not have been discovered yet and, given the universality of the effect, their search should not be restricted to oxides.

The many experimental observations discussed in this review clearly highlight the important role of flexoelectricity in the electromechanical properties of materials. At the same time, their interpretation in terms of flexoelectricity is often not straight forward. A number of findings, ranging from measurements of flexoelectricity in ceramics to some of the poling effects in ferroelectric and quasi-amorphous films, suggest values of bulk flexoelectric coefficients that greatly exceed the criteria for stability of these materials. A clarification of this issue is crucial to both our fundamental understanding and effective harvesting of flexoelectricity.

There have been predictions that flexoelectricity should enable record-breaking piezoelectric performance at the nanoscale. Yet direct evidence for these is still scarce; the truncated pyramid composites of Penn State [101] are probably not small enough, while the twinning-induced flexoelectric rotation of polarization [121] has not yet been complemented by a direct measurement of the expected concomitant piezoelectric enhancement due to the difficulties posed by the very reduced thickness of the epitaxially clamped samples. Meanwhile, the theoretical nanocantilevers with record piezoelectric performance proposed by the group of Sharma *et al.* have not been experimentally realized, though recent developments in the fabrication of nanotubes, nanorods and other nanoscale objects could make this a reality in the near future. At present, the only devices that appear to be delivering impressive performances are the flexural composites made at Penn State shown in **Figure 9a** [105]. We foresee that within the applied physics and materials engineering community there will continue to be strong drive to demonstrate the role of flexoelectricity in improved electromechanical energy harvesting. It is also likely that the recent discovery of flexoelectric switching of polarization [25] will inspire further research on the mechanical control of polarity.

There are also other, perhaps more peripheral but equally inspiring subjects for the more adventurous scientists (see special topic box). Flexomagnetism has been theoretically proposed, but there is no conclusive proof of its existence or its magnitude, nor of its applications. Large strain gradients inside domain walls or near dislocations should also lead to enormous flexoelectric effects that have not received much attention.

The above are but a few suggestions, but this review does not aim to be prescriptive. Rather, we would like to finish by reiterating the reasons why we think

flexoelectricity is important and likely to grow. It is a universal property of all materials irrespective of symmetry or composition, and this includes magnetic and biological materials. It is moreover an effect that grows as device size diminishes, being large at the nanoscale and therefore important for understanding and manipulating the properties of nanodevices. And last, but not least, it is, as we hope to have shown, still a work in progress, and there are few things more stimulating to a scientist than an unresolved problem.

8 Acknowledgements

The authors are indebted to Dragan Damjanovic, John F. Fu and Max Stengel for illuminating discussions. The authors also gratefully acknowledge funding from the Swiss National Science Foundation (A.K.T. and P.Z.) and from the Leverhulme Trust (G.C. and P.Z.).

Literature Cited

1. É. V. Bursian and O. I. Zaikovskii. Changes in the curvature of a ferroelectric film due to polarization. *Sov. Phys. Solid State*, 10(5):1121–1124, 1968.
2. Paul Harris. Mechanism for the shock polarization of dielectrics. *Journal of Applied Physics*, 36(3):739–741, 1965.
3. A. K. Tagantsev. Pyroelectric, piezoelectric, flexoelectric, and thermal polarization effects in ionic crystalss. *Soviet Physics Uspekhi*, 30:588–603, 1987.
4. Alexander K. Tagantsev. Electric polarization in crystals and its response to thermal and elastic perturbations. *Phase Transitions*, 35(3-4):119–203, 1991.

5. Sergei V. Kalinin and Vincent Meunier. Electronic flexoelectricity in low-dimensional systems. *Phys. Rev. B*, 77:033403, Jan 2008.

6. Robert B. Meyer. Piezoelectric effects in liquid crystals. *Phys. Rev. Lett.*, 22:918–921, 1969.

7. Alexander G. Petrov. Flexoelectricity of model and living membranes. *Biochimica et Biophysica Acta (BBA) - Biomembranes*, 1561(1):1 – 25, 2002.

8. A. G. Petrov. Electricity and mechanics of biomembrane systems: Flexoelectricity in living membranes. *Analytica Chimica Acta*, 568(1-2):70–83, 2006.

9. Kathryn D. Breneman, William E. Brownell, and Richard D. Rabbitt. Hair cell bundles: Flexoelectric motors of the inner ear. *PLoS ONE*, 4:e5201, 04 2009.

10. L. Cross. Flexoelectric effects: Charge separation in insulating solids subjected to elastic strain gradients. *Journal of Materials Science*, 41:53–63, 2006.

11. R. Maranganti, N. D. Sharma, and P. Sharma. Electromechanical coupling in nonpiezoelectric materials due to nanoscale nonlocal size effects: Green's function solutions and embedded inclusions. *Phys. Rev. B*, 74:014110, 2006.

12. Wenhui Ma. Flexoelectric charge separation and size dependent piezoelectricity in dielectric solids. *physica status solidi (b)*, 247(1):213–218, 2010.

13. V. S. Mashkevich and K. B. Tolpygo. Electrical, optical and elastic properties of diamond type crystals. i. *Soviet Physics JETP*, 5(3):435– 439, 1957.

14. K. B. Tolpygo. Long wavelength oscillations of diamond-type crystals including long range forces. *Soviet Physics - Solid State*, 4:1297–1305, 1963.

15. S. M. Kogan. Piezoelectric effect during inhomogeneous deformation and acoustic scattering of carriers in crystals. *Sov. Phys. Solid State*, 5(10):2069–2070, 1964.

16. A. K. Tagantsev. Piezoelectricity and flexoelectricity in crystalline dielectrics. *Phys. Rev. B*, 34:5883–5889, 1986.

17. Alexander K. Tagantsev, Eric Courtens, and Ludovic Arzel. Prediction of a low-temperature ferroelectric instability in antiphase domain boundaries of strontium titanate. *Phys. Rev. B*, 64:224107, 2001.

18. G. Catalan, L. J. Sinnamon, and J. M. Gregg. The effect of flexoelectricity on the dielectric properties of inhomogeneously strained ferroelectric thin films. *Journal of Physics: Condensed Matter*, 16(13):2253, 2004.

19. Anna N. Morozovska, Eugene A. Eliseev, Maya D. Glinchuk, Long-Qing Chen, and Venkatraman Gopalan. Interfacial polarization and pyroelectricity in antiferrodistortive structures induced by a flexoelectric effect and rotostriction. *Phys. Rev. B*, 85:094107, Mar 2012.

20. A. F. Devonshire. Theory of barium titanate. *Philosophical Magazine*, 40(309):1040–1063, 1949.

21. R.D. and Mindlin. Polarization gradient in elastic dielectrics. *International Journal of Solids and Structures*, 4(6):637 – 642, 1968.

22. A. Gruverman, B. J. Rodriguez, A. I. Kingon, R. J. Nemanich, A. K. Tagantsev, J. S. Cross, and M. Tsukada. Mechanical stress effect on imprint behavior of integrated ferroelectric capacitors. *Applied Physics Letters*, 83(4):728–730, 2003.

23. Wenhui Ma. A study of flexoelectric coupling associated internal electric field and stress in thin film ferroelectrics. *physica status solidi (b)*,

245(4):761–768, 2008.

24. D. Lee, A. Yoon, S. Y. Jang, J.-G. Yoon, J.-S. Chung, M. Kim, J. F. Scott, and T. W. Noh. Giant flexoelectric effect in ferroelectric epitaxial thin films. *Phys. Rev. Lett.*, 107:057602, 2011.

25. H. Lu, C.-W. Bark, D. Esque de los Ojos, J. Alcala, C. B. Eom, G. Catalan, and A. Gruverman. Mechanical writing of ferroelectric polarization. *Science*, 336(6077):59–61, 2012.

26. J. D. Axe, J. Harada, and G. Shirane. Anomalous acoustic dispersion in centrosymmetric crystals with soft optic phonons. *Phys. Rev. B*, 1:1227–1234, 1970.

27. Yu. I. Sirotin and M.P. Shaskolskaya. *Fundamentals of Crystal Physics*. Mir, Moscow, 1982.

28. H. Le Quang and Q.-C. He. The number and types of all possible rotational symmetries for flexoelectric tensors. *Proceedings of the Royal Society A: Mathematical, Physical and Engineering Science*, pages 1–18, 2011.

29. Longlong Shu, Xiaoyong Wei, Ting Pang, Xi Yao, and Chunlei Wang. Symmetry of flexoelectric coefficients in crystalline medium. *Journal of Applied Physics*, 110(10):104106, 2011.

30. Alexander K. Tagantsev and Alexander S. Yurkov. Flexoelectric effect in finite samples. *Journal of Applied Physics*, 112(4):044103–7, 2012.

31. É. V. Bursian and N. N. Trunov. Nonlocal piezoelectric effect. *Sov. Phys. Solid State*, 10:760–762, 1974.

32. Eugene A. Eliseev, Anna N. Morozovska, Maya D. Glinchuk, and R. Blinc. Spontaneous flexoelectric/flexomagnetic effect in nanoferroics. *Phys. Rev. B*, 79:165433, 2009.

33. A. Yurkov. Elastic boundary conditions in the presence of the flexoelectric effect. *JETP Letters*, 94:455–458, 2011.

34. A. Klíč and M. Marvan. Theoretical study of the flexoelectric effect based on a simple model of ferroelectric material. *Integrated Ferroelectrics*, 63(1):155–159, 2004.

35. A. Askar, P. C. Y. Lee, and A. S. Cakmak. Lattice-dynamics approach to the theory of elastic dielectrics with polarization gradient. *Physical Review B*, 1(8):3525, 1970.

36. Raffaele Resta. Towards a bulk theory of flexoelectricity. *Phys. Rev. Lett.*, 105:127601, 2010.

37. Jiawang Hong and David Vanderbilt. First-principles theory of frozen-ion flexoelectricity. *Phys. Rev. B*, 84:180101, 2011.

38. R. M. Martin. Piezoelectricity. *Physical Review B*, 5(4):1607, 1972.

39. Max Born and Kun Huang. *Dynamical Theory of Crystal Lattices*. Oxford University Press, Oxford, 1962.

40. R. Maranganti and P. Sharma. Atomistic determination of flexoelectric properties of crystalline dielectrics. *Phys. Rev. B*, 80:054109, 2009.

41. Jiawang Hong, G Catalan, J F Scott, and E Artacho. The flexoelectricity of barium and strontium titanates from first principles. *Journal of Physics: Condensed Matter*, 22(11):112201, 2010.

42. I. Ponomareva, A. K. Tagantsev, and L. Bellaiche. Finite-temperature flexoelectricity in ferroelectric thin films from first principles. *Phys. Rev. B*, 85:104101, 2012.

43. T. Dumitrica, C. M. Landis, and B. I. Yakobson. Curvature-induced polarization in carbon nanoshells. *Chemical Physics Letters*, 360(1-2):182–188,

2002.

44. T. Ibe. Bending piezoelectricity in polytetrafluoroethylene. *Japanese Journal of Applied Physics*, 13:197–198, 1974.

45. L. Breger, T. Furukawa, and E. Fukada. Bending piezoelectricity in polyvinylidene fluoride. *Japanese Journal of Applied Physics*, 15:2239–2240, 1976.

46. E. Fukada, G. M. Sessler, J. E. West, A. Berraissoul, and P. Günther. Bending piezoelectricity in monomorph polymer films. *Journal of Applied Physics*, 62:3643–3646, 1987.

47. Wenhui Ma and L. Eric Cross. Observation of the flexoelectric effect in relaxor $Pb(Mg_{1/3}Nb_{2/3})O_3$ ceramics. *Applied Physics Letters*, 78(19):2920–2921, 2001.

48. Wenhui Ma and L. Eric Cross. Large flexoelectric polarization in ceramic lead magnesium niobate. *Applied Physics Letters*, 79(26):4420–4422, 2001.

49. Wenhui Ma and L. Eric Cross. Flexoelectric polarization of barium strontium titanate in the paraelectric state. *Applied Physics Letters*, 81(18):3440–3442, 2002.

50. Wenhui Ma and L. Eric Cross. Flexoelectric effect in ceramic lead zirconate titanate. *Applied Physics Letters*, 86(7):072905, 2005.

51. Wenhui Ma and L. Eric Cross. Flexoelectricity of barium titanate. *Applied Physics Letters*, 88(23):232902, 2006.

52. Wenhui Ma and L. Eric Cross. Strain-gradient-induced electric polarization in lead zirconate titanate ceramics. *Applied Physics Letters*, 82(19):3293–3295, 2003.

53. P. Zubko, G. Catalan, A. Buckley, P. R. L. Welche, and J. F. Scott. Strain-

gradient-induced polarization in $SrTiO_3$ single crystals. *Phys. Rev. Lett.*, 99:167601, 2007.

54. P. Zubko, G. Catalan, A. Buckley, P. R. L. Welche, and J. F. Scott. Erratum: Strain-gradient-induced polarization in $SrTiO_3$ single crystals [phys. rev. lett. 99, 167601 (2007)]. *Phys. Rev. Lett.*, 100:199906, 2008.

55. Sivapalan Baskaran, Xiangtong He, Qin Chen, and John Y. Fu. Experimental studies on the direct flexoelectric effect in alpha-phase polyvinylidene fluoride films. *Applied Physics Letters*, 98(24):242901, 2011.

56. John Y. Fu, Wenyi Zhu, Nan Li, and L. Eric Cross. Experimental studies of the converse flexoelectric effect induced by inhomogeneous electric field in a barium strontium titanate composition. *Journal of Applied Physics*, 100(2):024112, 2006.

57. P. Hana, M. Marvan, L. Burianova, S. J. Zhang, E. Furman, and T. R. Shrout. Study of the inverse flexoelectric phenomena in ceramic lead magnesium niobate-lead titanate. *Ferroelectrics*, 336:137–144, 2006.

58. P. Hana. Study of flexoelectric phenomenon from direct and from inverse flexoelectric behavior of pmnt ceramic. *Ferroelectrics*, 351:196–203, 2007.

59. V.G. Vaks. *Introduction to the Microscopic Theory of Ferroelectrics*. Nauka, Moscow, 1973.

60. J. Harada, J. Axe, and G. Shirane. Neutron-scattering study of soft modes in cubic batio3. *Phys. Rev.B*, 4:155, 1971.

61. E. Farhi, A. K. Tagantsev, R. Currat, B. Hehlen, E. Courtens, and L. A. Boatner. Low energy phonon spectrum and its parameterization in pure ktao3 below 80 k. *European Physical Journal B*, 15(4):615–623, 2000.

62. Sivapalan Baskaran, Narayanan Ramachandran, Xiangtong He, Sankar

Thiruvannamalai, Ho Joon Lee, Hyun Heo, Qin Chen, and John Y. Fu. Giant flexoelectricity in polyvinylidene fluoride films. *Physics Letters A*, 375(20):2082 – 2084, 2011.

63. Sivapalan Baskaran, Xiangtong He, Yu Wang, and John Y. Fu. Strain gradient induced electric polarization in alpha -phase polyvinylidene fluoride films under bending conditions. *Journal of Applied Physics*, 111(1):014109, 2012.

64. M. Marvan and A. Havránek. Flexoelectric effect in elastomers. *Progr. Colloid Polym. Sci.*, 78:33–36, 1988.

65. B. Chu and D. R. Salem. Flexoelectricity in several thermoplastic and thermosetting polymers. *Applied Physics Letters*, 101:103905, 2012.

66. J. W. Matthews and A. E. Blakeslee. Defects in epitaxial multilayers: I. Misfit dislocations. *Journal of Crystal Growth*, 27:118 – 125, 1974.

67. G. Catalan, B. Noheda, J. McAneney, L. J. Sinnamon, and J. M. Gregg. Strain gradients in epitaxial ferroelectrics. *Phys. Rev. B*, 72:020102, 2005.

68. H. Joon Kim, S. Hoon Oh, and Hyun M. Jang. Thermodynamic theory of stress distribution in epitaxial Pb(Zr, Ti)O_3 thin films. *Applied Physics Letters*, 75(20):3195–3197, 1999.

69. M. S. Majdoub, R. Maranganti, and P. Sharma. Understanding the origins of the intrinsic dead layer effect in nanocapacitors. *Phys. Rev. B*, 79:115412, 2009.

70. L. J. Sinnamon, R. M. Bowman, and J. M. Gregg. Investigation of dead-layer thickness in $SrRuO_3/Ba_{0.5}Sr_{0.5}TiO_3$/Au thin-film capacitors. *Applied Physics Letters*, 78(12):1724–1726, 2001.

71. Hao Zhou, Jiawang Hong, Yihui Zhang, Faxin Li, Yongmao Pei, and Dain-

ing Fang. Flexoelectricity induced increase of critical thickness in epitaxial ferroelectric thin films. *Physica B: Condensed Matter*, 407(17):3377 – 3381, 2012.

72. J. F. Scott. Lattice perturbationsin $CaWO_4$ and $CaMoO_4$. *Journal of Chemical Physics*, 48:874, 1968.

73. Andrei Kholkin, Igor Bdikin, Tetyana Ostapchuk, and Jan Petzelt. Room temperature surface piezoelectricity in srtio[sub 3] ceramics via piezoresponse force microscopy. *Applied Physics Letters*, 93(22):222905, 2008.

74. V. Lyahovitskaya, Y. Feldman, I. Zon, E. Wachtel, K. Gartsman, A. K. Tagantsev, and I. Lubomirsky. Formation and thermal stability of quasi-amorphous thin films. *Phys. Rev. B*, 71:094205, 2005.

75. A. K. Tagantsev, L. E. Cross, and J. Fousek. *Domains in Ferroic Crystals and Thin Films*. Springer, New York, 2010.

76. E. V. Bursian, Zaikovsk.Oi, and K. V. Makarov. Ferroelectric plate polarization by bending. *Izvestiya Akademii Nauk Sssr Seriya Fizicheskaya*, 33(7):1098–1102, 1969.

77. B. Hehlen, L. Arzel, A. K. Tagantsev, E. Courtens, Y. Inaba, A. Yamanaka, and K. Inoue. Brillouin-scattering observation of the ta-to coupling in $srtio_3$. *Physical Review B*, 57(22):R13989–R13992, 1998. PRB.

78. M. Gharbi, Z. H. Sun, P. Sharma, and K. White. The origins of electromechanical indentation size effect in ferroelectrics. *Applied Physics Letters*, 95(14):142901, 2009.

79. M. Gharbi, Z.H. Sun, P. Sharma, K. White, and S. El-Borgi. Flexoelectric properties of ferroelectrics and the nanoindentation size-effect. *International Journal of Solids and Structures*, 48(2):249–256, 2011.

80. C. R. Robinson, K. W. White, and P. Sharma. Elucidating the mechanism for indentation size-effect in dielectrics. *Applied Physics Letters*, 101(12):122901, 2012.

81. P. Aguado-Puente and J. Junquera. Structural and energetic properties of domains in $PbTiO_3/SrTiO_3$ superlattices from first principles. *Physical Review B*, 85:184105, 2012.

82. É. V. Bursian. The importance of the unlocal piezoeffect in domain structure formation in ferroelectrics. *Ferroelectrics*, 307(1):177–179, 2004.

83. P. Zubko, N. Jecklin, A. Torres-Pardo, P. Aguado-Puente, A. Gloter, C. Lichtensteiger, J. Junquera, and J.-M. Triscone. Electrostatic coupling and local structural distortions at interfaces in ferroelectric/paraelectric superlattices. *Nano Letters*, 12:2846–2851, 2012.

84. P. Zubko, S. Gariglio, M. Gabay, P. Ghosez, and J.-M. Triscone. Interface physics in complex oxide heterostructures. *Annual Review of Condensed Matter Physics*, 2:141–165, 2011.

85. Manuel Bibes, Javier Villegas, and Agnes Barthelemy. Ultrathin oxide films and interfaces for electronics and spintronics. *Advances In Physics*, 60:5–84, 2011.

86. G. Catalan, J. Seidel, R. Ramesh, and J. F. Scott. Domain wall nanoelectronics. *Rev. Mod. Phys.*, 84:119–156, Feb 2012.

87. Ekhard Salje and Huali Zhang. Domain boundary engineering. *Phase Transit.*, 82:452–469, 2009.

88. Farrel W. Lytle. X-ray diffractometry of low-temperature phase transformations in strontium titanate. *Journal of Applied Physics*, 35(7):2212–2215, 1964.

89. Wenwu Cao and Gerhard R. Barsch. Landau-ginzburg model of interphase boundaries in improper ferroelastic perovskites of d_{4h}^{18} symmetry. *Phys. Rev. B*, 41:4334–4348, 1990.

90. J. F. Scott, E. K. H. Salje, and M. A. Carpenter. Domain wall damping and elastic softening in $SrTiO_3$: Evidence for polar twin walls. *Physical Review Letters*, page in press, 2012.

91. A. V. Kityk, W. Schranz, P. Sondergeld, D. Havlik, E. K. H. Salje, and J. F. Scott. Low-frequency superelasticity and nonlinear elastic behavior of $srtio_3$ crystals. *Phys. Rev. B*, 61:946–956, Jan 2000.

92. R. J. Zeches, M. D. Rossell, J. X. Zhang, A. J. Hatt, Q. He, C.-H. Yang, A. Kumar, C. H. Wang, A. Melville, C. Adamo, G. Sheng, Y.-H. Chu, J. F. Ihlefeld, R. Erni, C. Ederer, V. Gopalan, L. Q. Chen, D. G. Schlom, N. A. Spaldin, L. W. Martin, and R. Ramesh. A strain-driven morphotropic phase boundary in $BiFeO_3$. *Science*, 326:977–980, 2009.

93. J. X. Zhang, R. J. Zeches, Q. He, Y.-H. Chu, and R. Ramesh. Nanoscale phase boundary: a new twist to novel functionalities. *Nanoscale*, in press.

94. Pavel Lukashev and Renat F. Sabirianov. Flexomagnetic effect in frustrated triangular magnetic structures. *Phys. Rev. B*, 82:094417, 2010.

95. J. Seidel, L. W. Martin, Q. He, Q. Zhan, Y. H. Chu, A. Rother, M. E. Hawkridge, P. Maksymovych, P. Yu, M. Gajek, N. Balke, S. V. Kalinin, S. Gemming, F. Wang, G. Catalan, J. F. Scott, N. A. Spaldin, J. Orenstein, and R. Ramesh. Conduction at domain walls in oxide multiferroics. *Nat. Mater.*, 8:229–234, 2009.

96. E. A. Eliseev, M. D. Glinchuk, V. Khist, V. V. Skorokhod, R. Blinc, and A. N. Morozovska. Linear magnetoelectric coupling and ferroelectricity in-

duced by the flexomagnetic effect in ferroics. *Phys. Rev. B*, 84:174112, 2011.

97. Peter Maksymovych, Anna N. Morozovska, Pu Yu, Eugene A. Eliseev, Ying-Hao Chu, Ramamoorthy Ramesh, Arthur P. Baddorf, and Sergei V. Kalinin. Tunable metallic conductance in ferroelectric nanodomains. *Nano Letters*, 12(1):209–213, 2012.

98. A. Y. Borisevich, E. A. Eliseev, A. N. Morozovska, C.-J. Cheng, J.-Y. Lin, Y. H. Chu, D. Kan, I. Takeuchi, V. Nagarajan, and S. V. Kalinin. Hatomic-scale evolution of modulated phases at the ferroelectricantiferroelectric morphotropic phase boundary controlled by flexoelectric interaction. *Nature Communications*, 3:775, 2012.

99. S. J. Ahn, J.-J. Kim, J-H. Kim, and W-K. Choo. Origin of polar domains in ferroelectric relaxors. *J. Korean Phys. Soc*, 42:S1009–S1011, 2003.

100. J. Fousek, L.E. Cross, and D.B. Litvin. Possible piezoelectric composites based on the flexoelectric effect. *Materials Letters*, 39(5):287–291, 1999.

101. John Y. Fu, Wenyi Zhu, Nan Li, Nadine B. Smith, and L. Eric Cross. Gradient scaling phenomenon in microsize flexoelectric piezoelectric composites. *Applied Physics Letters*, 91(18):182910, 2007.

102. Wenyi Zhu, John Y. Fu, Nan Li, and L. Cross. Piezoelectric composite based on the enhanced flexoelectric effects. *Applied Physics Letters*, 89(19):192904, 2006.

103. N.D. Sharma, R. Maranganti, and P. Sharma. On the possibility of piezoelectric nanocomposites without using piezoelectric materials. *Journal of the Mechanics and Physics of Solids*, 55(11):2328 – 2350, 2007.

104. Swapnil Chandratre and Pradeep Sharma. Coaxing graphene to be piezoelectric. *Applied Physics Letters*, 100(2):023114, 2012.

105. Baojin Chu, Wenyi Zhu, Nan Li, and L. Eric Cross. Flexure mode flexoelectric piezoelectric composites. *Journal of Applied Physics*, 106(10):104109, 2009.

106. M. S. Majdoub, P. Sharma, and T. Çağin. Dramatic enhancement in energy harvesting for a narrow range of dimensions in piezoelectric nanostructures. *Phys. Rev. B*, 78:121407, 2008.

107. I. Szafraniak, C. Harnagea, R. Scholz, S. Bhattacharyya, D. Hesse, and M. Alexe. Ferroelectric epitaxial nanocrystals obtained by a self-patterning method. *Applied Physics Letters*, 83(11):2211–2213, 2003.

108. Hajime Nonomura, Masaki Nagata, Hironori Fujisawa, Masaru Shimizu, Hirohiko Niu, and Koichiro Honda. Structural control of self-assembled $PbTiO_3$ nanoislands fabricated by metalorganic chemical vapor deposition. *Applied Physics Letters*, 86(16):163106, 2005.

109. Z. L. Wang and J. Song. Piezoelectric nanogenerators based on zinc oxide nanowire arrays. *Science*, 312:242–246, 2006.

110. H. N. Lee, H. M. Christen, M. F. Chisholm, C.M. Rouleau, and D. H. Lowndes. Strong polarization enhancement in asymmetric three-component ferroelectric superlattices. *Nature*, 433:395–399, 2005.

111. Yi Qi, Jihoon Kim, Thanh D. Nguyen, Bozhena Lisko, Prashant K. Purohit, and Michael C. McAlpine. Enhanced piezoelectricity and stretchability in energy harvesting devices fabricated from buckled pzt ribbons. *Nano Letters*, 11(3):1331–1336, 2011.

112. Stephen S. Nonnenmann, Oren D. Leaffer, Eric M. Gallo, Michael T. Coster, and Jonathan E. Spanier. Finite curvature-mediated ferroelectricity. *Nano Letters*, 10(2):542–546, 2010.

113. D. G. Schlom, L.-Q. Chen, C.-B. Eom, K. M. Rabe, S. K. Streiffer, and J.-M. Triscone. Strain tuning of ferroelectric thin films. *Annu. Rev. Mater. Res.*, 37:589–626, 2007.

114. J.-P. Locquet, J. Perret, J. Fompeyrine, E. Mächler, J. W. Seo, and G. Van Tendeloo. Doubling the critical temperature of $La_{1.9}Sr_{0.1}CuO_4$ using epitaxial strain. *Nature*, 394:453–456, 1998.

115. J. H. Haeni, P. Irvin, W. Chang, R. Uecker, P. Reiche, Y. L. Li, S. Choudhury, W. Tian, M. E. Hawley, B. Craigo, A. K. Tagantsev, X. Q. Pan, S. K. Streiffer, L. Q. Chen, S. W. Kirchoefer, J. Levy, and D. G. Schlom. Room-temperature ferroelectricity in strained $SrTiO_3$. *Nature*, 430:758–761, 2004.

116. N. D. Sharma, C. M. Landis, and P. Sharma. Piezoelectric thin-film superlattices without using piezoelectric materials. *Journal of Applied Physics*, 108(2):024304, 2010.

117. Z.-G. Ban, S. P. Alpay, and J. V. Mantese. Fundamentals of graded ferroic materials and devices. *Phys. Rev. B*, 67:184104, 2003.

118. N. Sai, B. Meyer, and D. Vanderbilt. Compositional inversion symmetry breaking in ferroelectric perovskites. *Phys. Rev. Lett.*, 84:5636–5639, 2000.

119. J. S. Speck and W. Pompe. Domain configurations due to multiple misfit relaxation mechanisms in epitaxial ferroelectric thin films. I. Theory. *Journal of Applied Physics*, 76(1):466–476, 1994.

120. J. S. Speck, A. Seifert, W. Pompe, and R. Ramesh. Domain configurations due to multiple misfit relaxation mechanisms in epitaxial ferroelectric thin films. II. Experimental verification and implications. *Journal of Applied Physics*, 76(1):477–483, 1994.

121. G. Catalan, A. Lubk, A. H. G. Vlooswijk, E. Snoeck, C. Magen, A. Janssens,

G. Rispens, G. Rijnders, D. H. A. Blank, and B. Noheda. Flexoelectric rotation of polarization in ferroelectric thin films. *Nature Materials*, 10:963967, 2005.

122. A. N. Morozovska, E. A. Eliseev, A. K. Tagantsev, S. L. Bravina, Long-Qing Chen, and S. V. Kalinin. Thermodynamics of electromechanically coupled mixed ionic-electronic conductors: Deformation potential, vegard strains, and flexoelectric effect. *Phys. Rev. B*, 83:195313, May 2011.

123. A. P. Pyatkov and A. K. Zvezdin. Flexomagnetoelectric interaction in multiferroics. *Eur. Phys. J. B*, 71:419–427, 2009.

124. A. K. Zvezdin and A. A. Mukhin. On the effect of inhomogeneous magnetoelectric (flexomagnetoelectric) interaction on the spectrum and properties of magnons in multiferroics. *JETP Letters*, 89(7):328–332, 2009.

125. Wenbin Huang, Kyungrim Kim, Shujun Zhang, Fuh-Gwo Yuan, and Xiaoning Jiang. Scaling effect of flexoelectric (ba,sr)tio3 microcantilevers. *physica status solidi (RRL) Rapid Research Letters*, 5(9):350–352, 2011.

126. R. A. Cowley. Lattice dynamics and phase transitions of strontium titanate. *Physical Review*, 134(4A):A981–A997, 1964. PR.

127. S. M. Shandarov, S. S. Shmakov, N. I. Burimov, O. S. Syuvaeva, Y. F. Kargin, and V. M. Petrov. Detection of the contribution of the inverse flexoelectric effect to the photorefractive response in a bismuth titanium oxide single crystal. *Jetp Letters*, 95(12):618–621, 2012.

Definitions

Piezoelectricity— linear response of polarization to mechanical strain and vice versa; possible only in noncentrosymmetric materials.

Electrostriction— contribution to the strain proportional to the square of the polarization (or the square of an external electric field); possible in any material.

Ferroelectric—piezoelectric material whose piezoelectric tensor's sign can be reversed by an external electric field.

(To be placed in the introduction, where the terms are first mentioned.)

Sidebar

Flexomagnetism

Symmetry-wise, the same coupling between strain gradient and polarization is also allowed between strain gradient and magnetization [32]. The direct flexomagnetic effect has been theoretically postulated by Lukashev and Sabirianov [94]. An indirect flexomagnetic effect must also be present in all magnetoelectrics: since in these materials polarization and magnetization are coupled, any gradient-induced polarization must indirectly induce some magnetization [123, 124].

(To be placed close to section 5.2.5, where it is first mentioned)

Ceramics					
Compound	Coefficient	Method	Value (μC/m)	χ/ϵ_0	$f = \mu/$
$BaTiO_3$	$\tilde{\mu}_{12}(T_c + 3.4\ \mathrm{K})$	CB	50 [51]		∼540
$Ba_{0.67}Sr_{0.33}TiO_3$	$\tilde{\mu}_{11}$	PC (0.5 Hz)	150 [10]	∼20000	∼8
	$\tilde{\mu}_{11}$	CFE (400 Hz)	120 [56]		
	$\tilde{\mu}_{12}$	CB (1 Hz)	100 [49]		∼4
$Ba_{0.65}Sr_{0.35}TiO_3$	$\tilde{\mu}_{12}$	CB	∼ 80 [125]	4100	23
$PbMg_{0.33}Nb_{0.67}O_3$	$\tilde{\mu}_{12}$	CB	3–4 [47]	∼13000	∼26
PMN-PT	$\tilde{\mu}_{11}$	PC (0 Hz)	6–12 [58]	21000	∼32
		PC (4–10 Hz)	20–50 [58]		∼110
$Pb_{0.3}Sr_{0.7}TiO_3$	$\tilde{\mu}_{11}$	PC (0.5 Hz)	20 [10]	13000	17
$Pb(Zr,Ti)O_3$	$\tilde{\mu}_{12}$	4PB	0.5 [52]	∼ 2200	2
		CB (1 Hz)	1.4 [50]		7

Table 1: Measured experimental coefficients for perovskite ceramics in the paraelectric phase. Underlined values were calculated from the measured flexoelectric coefficient and the experimental dielectric susceptibilities. All values are room temperature values unless stated otherwise. Measurment techniques: CB = cantilever bending; PC = pyramid compression; CFE = converse flexoelectric effect; 4PB = four-point bending.

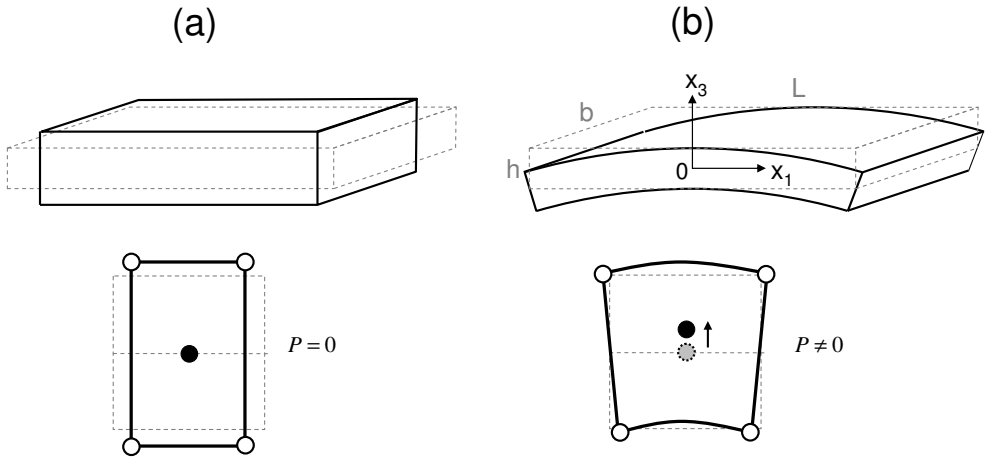

Figure 1: Cartoon illustrating the microscopic mechanism of flexoelectricity.

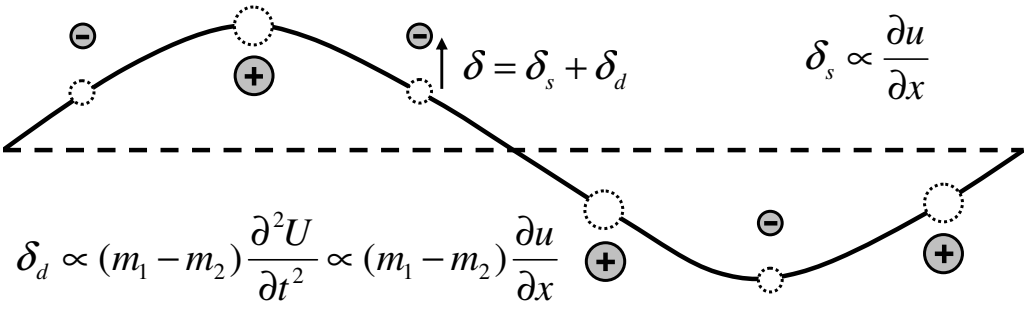

Figure 2: Illustration of the dynamic flexoelectric effect. An acoustic wave passing through a medium generates a time-dependent strain gradient which generates a polar displacement δ of the ions. For an acoustic wave, the acceleration of the atoms is proportional to the strain gradient and thus, on top of the static flexoelectric response $\delta_s \propto \frac{\partial u}{\partial x}$, the acceleration of ions of different masses gives rise to an additional polar displacement $\delta_d \propto (m_1 - m_2)\frac{\partial u}{\partial x}$.

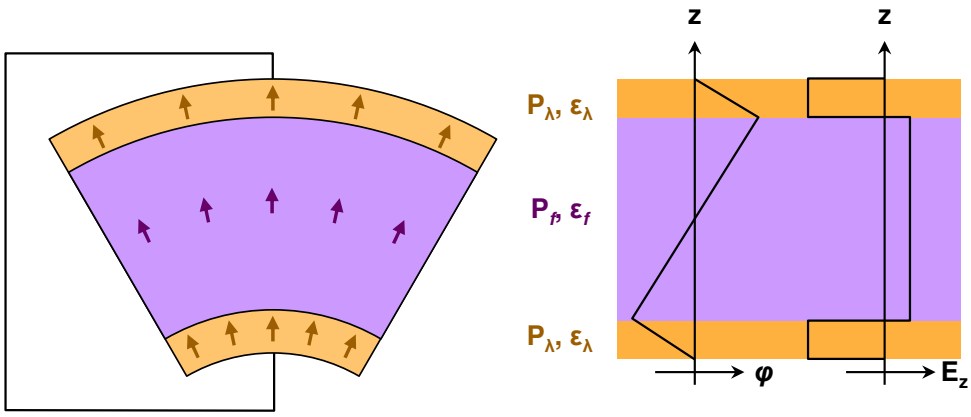

Figure 3: Surface piezoelectricity. Upon bending, the tensile/compressive strains in the top/bottom surface layers give rise to a polarization P_λ in a piezoelectric surface layer of thickness λ. Since the normal component of the electric displacement must remain constant, this surface polarization gives rise to electric fields E_b and thus a polarization P_b within the non-piezoelectric bulk. The measured average polarization of the whole structure therefore depends not only on the dielectric properties of the piezoelectric surface layers but also those of the bulk.

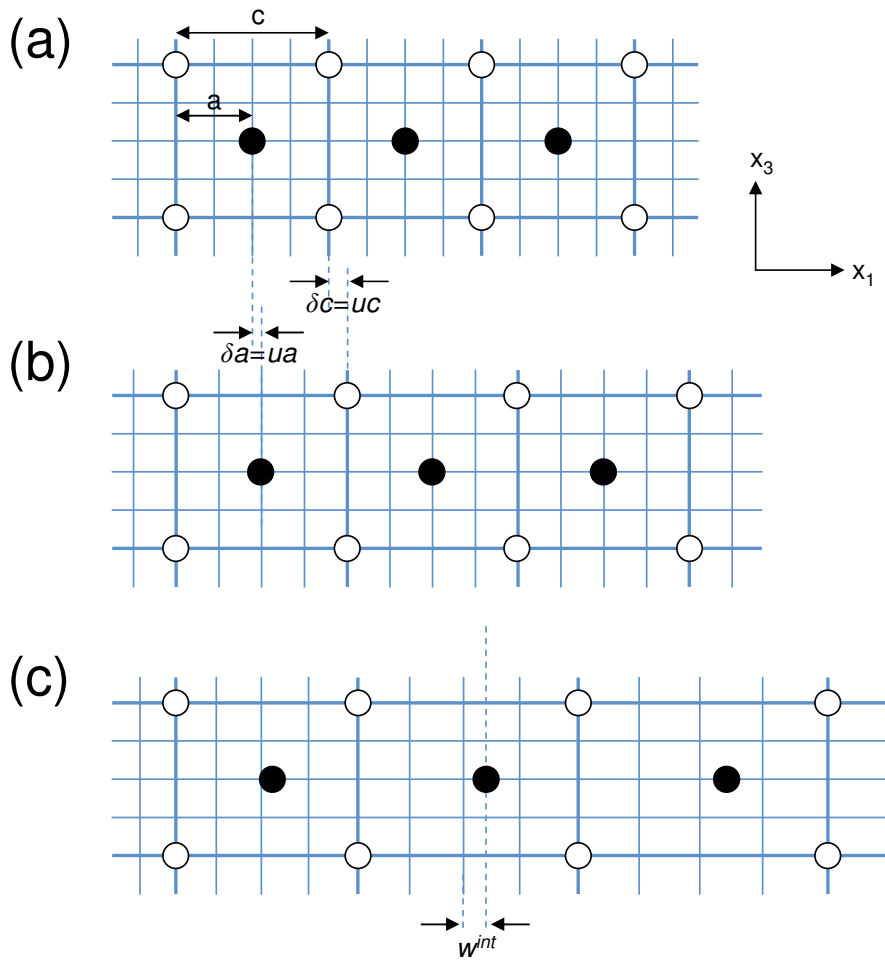

Figure 4: When uniformly strained along x_1, the centrosymmetric lattice in (a) will deform as shown in (b). All atomic displacements are restricted by symmetry and will follow the elastic medium approximation (blue lattice). For example, if the homogeneous strain is $u = u_{11}$, then $\delta c = uc$ and $\delta a = ua$. However, an inhomogeneous deformation, lifts this symmetry restriction, and the atomic displacements will not, in general, follow the elastic medium approximation (as shown for the black atoms in (c)). The difference w^{int} between the actual displacement (δa) and that expected from the elastic medium approximation (ua) gives rise to internal strain.

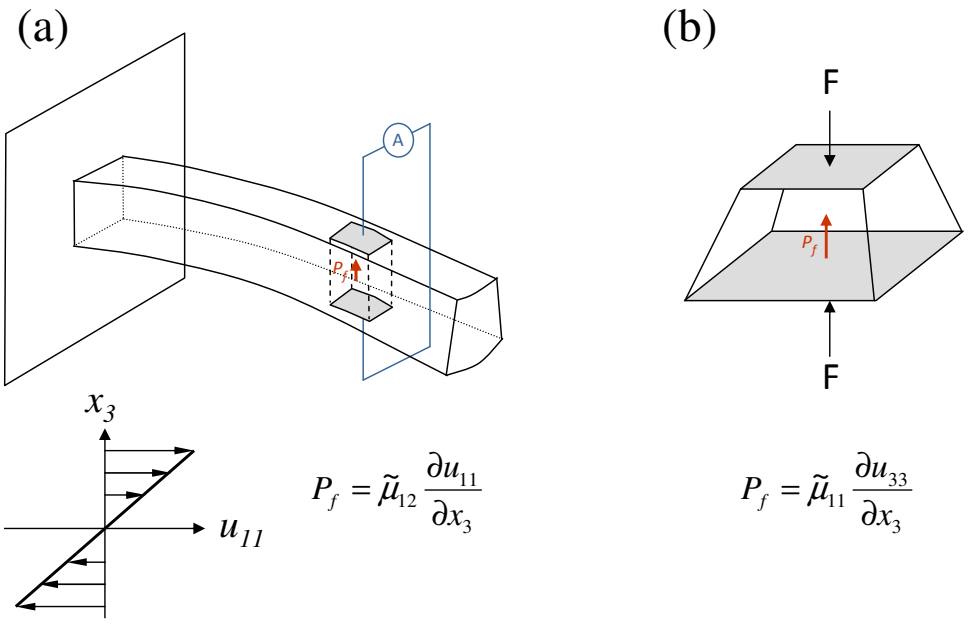

Figure 5: Methods most commonly used to quantify the flexoelectric response.

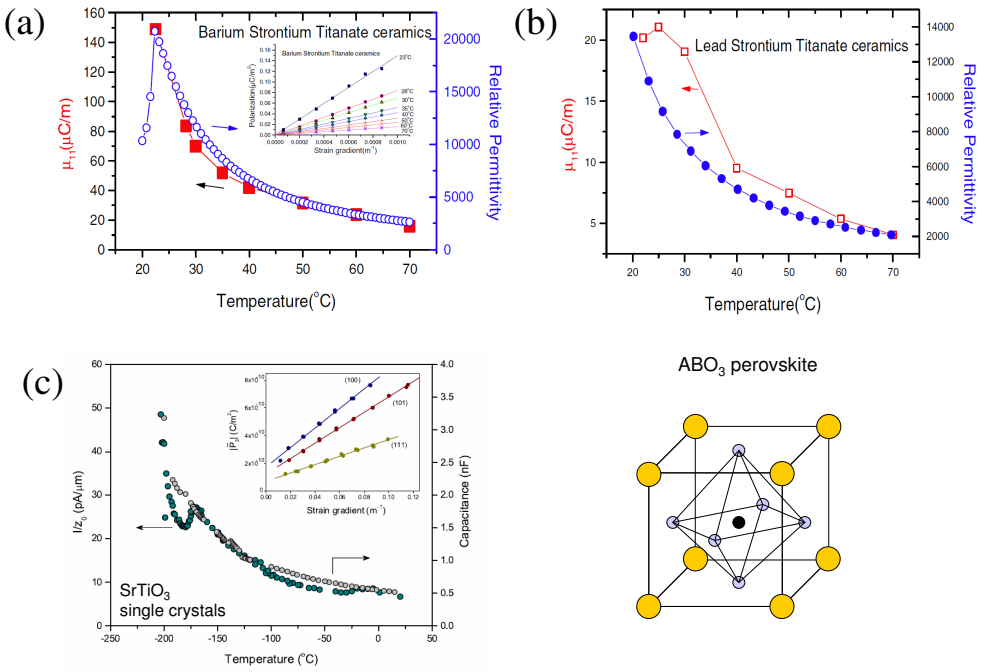

Figure 6: Temperature evolution of the effective longitudinal flexoelectric coefficient and the dielectric permittivity of (a) (Ba,Sr)TiO_3 and (b) (Pb,Sr)TiO_3 ceramics above the Curie temperature. Inset in (a) shows the linear relationship between polarization and strain gradient. (c) Temperature evolution of the ratio of flexoelectric current I and bending displacement z_0 (with $I/z_0 \propto \tilde{\mu}_{12}$) and dielectric constant of (100)-oriented crystal of $SrTiO_3$. The anomaly at ∼100 K is related to ferroelastic domain wall motion in $SrTiO_3$. The inset shows the linear relationship between polarization and strain gradients for three crystals of different orientation. (d) A sketch of the perovskite ABO_3 structure.

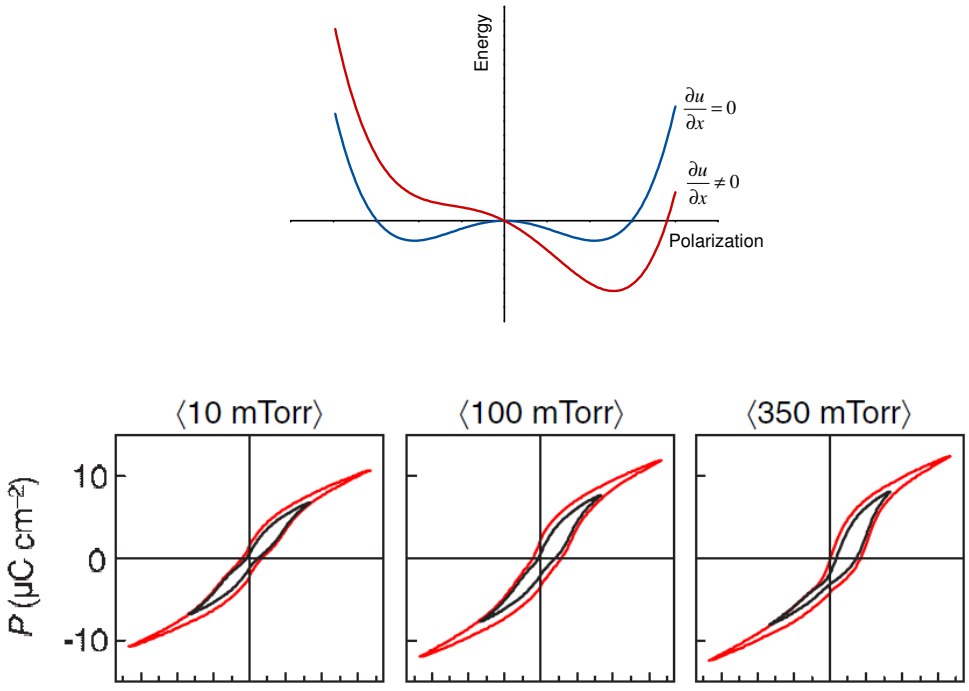

Figure 7: The effects of strain gradients in ferroelectric materials can mimic those of an electric field. Just like an electric field, a strain gradient leads to the skewing of the ferroelectric double-well potential, favoring one of the two polarization states. This can lead to imprint—a shift of the ferroelectric hysteresis loop along the field axis. In Ref. 24 progressively larger strain gradients were induced in $YMnO_3$ thin films by increasing the oxygen pressure during growth from 10 to 350 mTorr. The effective electric field due to these strain gradients interacts leads to a reorientation of defect dipoles which in turn cause the observed imprint once the samples are cooled to room temperature.

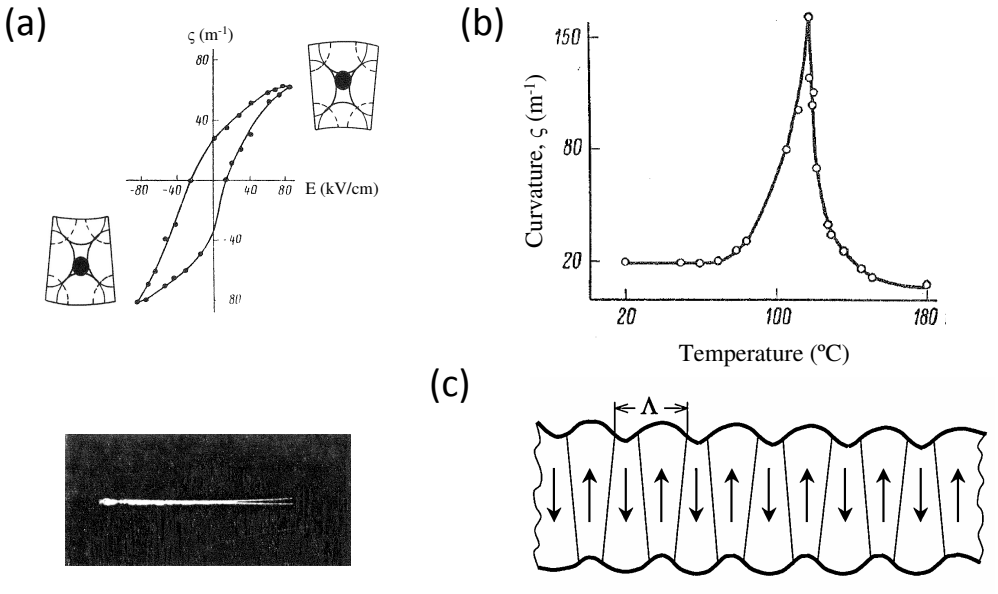

Figure 8: (a) Polarization-induced bending of a 2.5 μm-thick $BaTiO_3$ crystal in the ferroelectric phase at room temperature [1]. The sample curvature σ exhibits hysteresis due to the hysteretic response of the ferroelectric polarization. (b) Field-induced curvature as a function of temperature across the ferroelectric-to-paraelectric phase transition. (c) Local bending of a polydomain ferroelectric envisaged by Bursian [82].

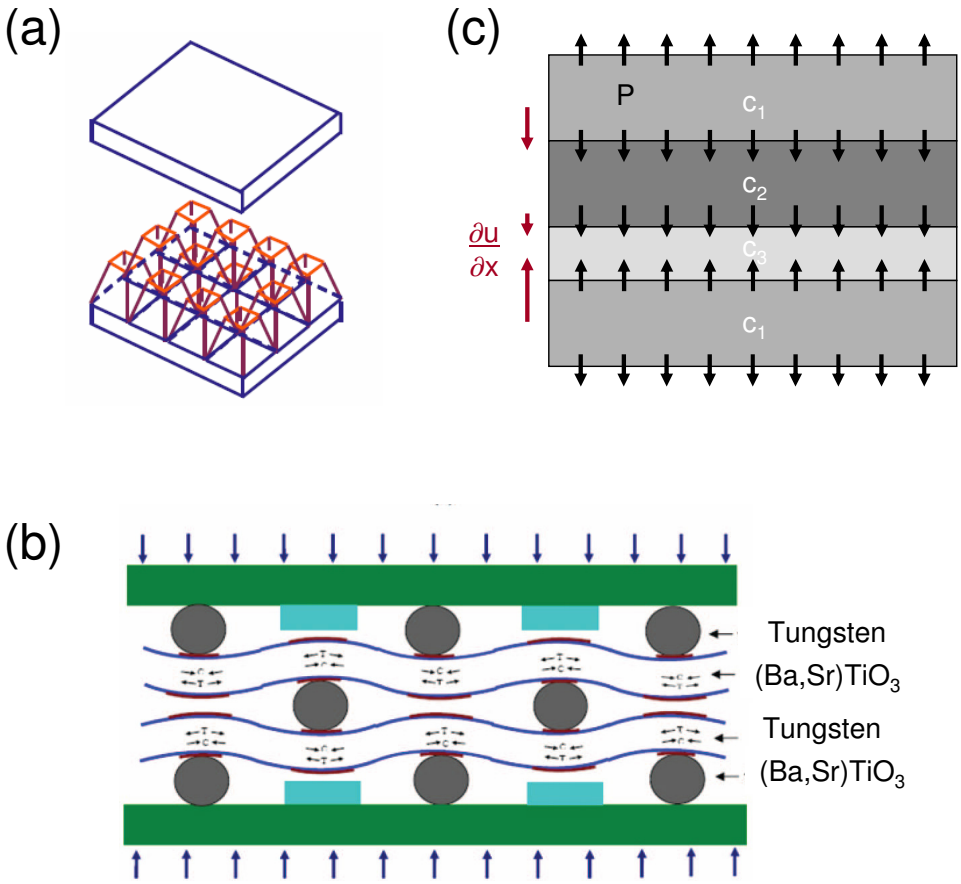

Figure 9: (a) Piezoelectric composite based on longitudinal flexoelectric effect. (b) Flexure-mode flexoelectric piezo-composite. (c) Piezoelectric composite based on interface flexoelectricity in a tri-color superlattice.

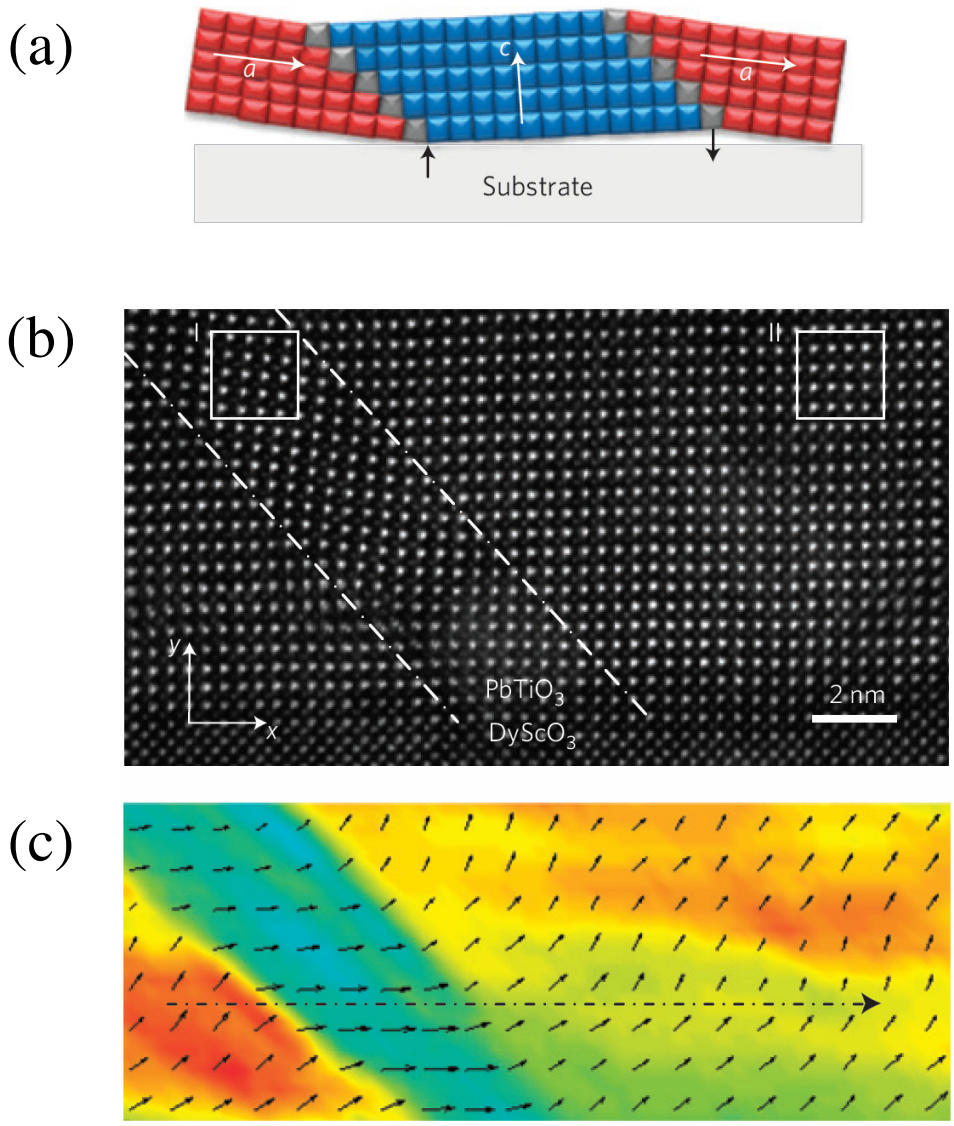

Figure 10: Epitaxial clamping of a ferroelastic film to a flat substrate, inhibits the natural distortions (a) of the ferroelastic domain structure and gives rise to a highly inhomogeneous strain distribution and therefore to flexoelectric polarization. High resolution transmission electron microscopy allows the positions of atoms to be determined with sub-Å resolution (b), and thus to map out the strain (color map in (c)) and polarization distributions (arrows in (c)) within the ferroelastic domains.

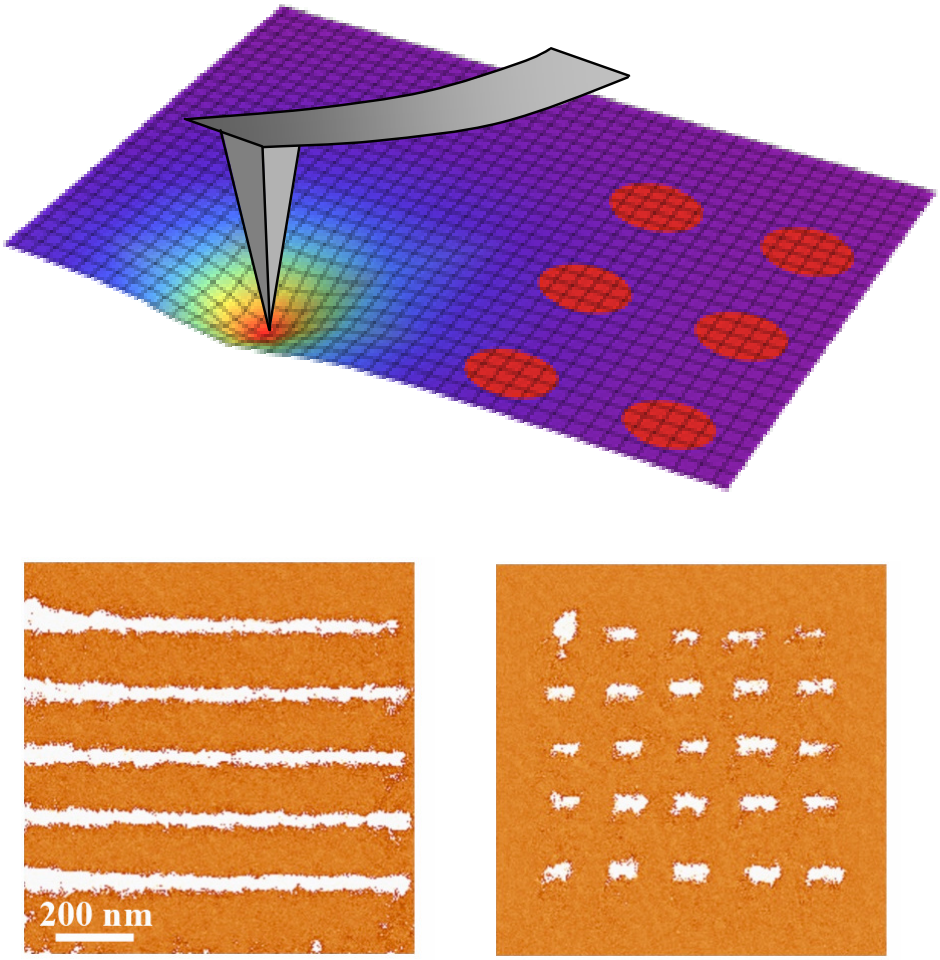

Figure 11: The "nanotypewriter". Highly concentrated stress fields under an AFM tip pressing on the sample surface produce strain gradients that are equivalent to an electric field sufficient to reverse the polarization of a ferroelectric thin film. Nanometric domains can thus be written by simple mechanical pressure, without any charge injection.

	μ_{44} (r.t.)	~5.8 [17, 54]		2.2	μ_{44}	3.6 [46]	
	$\mu_{11} - \mu_{12}$			(−1.2)–(+1.4) [59, 126]			
	μ_{44}			1.2–2; 2.4 [59, 77, 126]			
$KTaO_3$	$\mu_{11} - \mu_{12}$			0; 1.8 [26, 59, 61]			
	μ_{44}			2.9; 2.5 [26, 59, 61]			
$PbTiO_3$					μ_{11}		$-17^{(b)}$ [37]
$Bi_{12}TiO_{20}$	μ_{11} (r.t.)	5.3 [127]	47	12.5			
C			2.5–3		μ_{11}		$-20^{(b)}$ [37]
GaAs			12.5		μ_{11}	+0.51 $\times 10^{-2}$ [40]	0.046
						+0.85 $\times 10^{-2}$ [40]	0.077
					μ_{12}	-0.84 $\times 10^{-2}$ [40]	-0.076
						+0.50 $\times 10^{-2}$ [40]	0.045
					μ_{44}	+0.26 $\times 10^{-2}$ [40]	0.024
						+0.17 $\times 10^{-2}$ [40]	0.015
GaP			11.1		μ_{11}	+0.47 $\times 10^{-2}$ [40]	0.048
					μ_{12}	+0.31 $\times 10^{-2}$ [40]	0.022
					μ_{44}	-0.34 $\times 10^{-2}$ [40]	-0.034
ZnS			8.2		μ_{11}	-0.31 $\times 10^{-2}$ [40]	-0.043
					μ_{12}	-1.5 $\times 10^{-2}$ [40]	-0.021
					μ_{44}	-0.61 $\times 10^{-2}$ [40]	-0.084
KCl			4.6		μ_{11}	+0.40 $\times 10^{-2}$ [40]	0.098
					μ_{12}	-0.12 $\times 10^{-2}$ [40]	-0.030
					μ_{44}	-0.23 $\times 10^{-2}$ [40]	-0.057
MgO			9.7		μ_{11}		$-11^{(b)}$ [37]